

# CHAPTER 1

## INTRODUCTION

### 1.1 Background of Study

Pressure vessels used in industry are leak-tight pressure containers, usually cylindrical or spherical in shape, with different head configurations. They are usually made from carbon or stainless steel and assembled by welding.

Basic stress analysis calculations assume that the components are smooth, have a uniform section and no irregularities. In practice virtually all engineering components have to have changes in section and / or shape. Common examples are shoulders on shafts, oil holes, keys ways and screw threads. Any discontinuity changes the stress distribution in the vicinity of the discontinuity, so that the basic stress analysis equations no longer apply. Such 'discontinuities' or 'stress raisers' cause local increase of stress referred to as 'stress concentration'[1]. Geometric discontinuities cause an object to experience a local increase in the intensity of a stress field. The examples of shapes that cause these concentrations are: cracks, sharp corners, holes and, changes in the cross-sectional area of the object [2].

Stress concentration factor is the ratio of the highest stress to nominal stress of the cross-section. It is a function of the geometry and the applied loading of a structure. The project will cover the stress concentration factor at two adjacent nozzles in a thin-walled cylindrical pressure vessel."Thin wall" vessel refers to a vessel having an inner-radius-to-wall-thickness ratio of 10 or more ( $r/t \geq 10$ ).When the vessel wall is "thin", the stress distribution throughout its thickness will not vary significantly and it is assumed that it is uniform or constant. By using this assumption, the state of stress in thin-walled cylindrical pressure vessels can be analyzed.

## 1.2 Problem Statement

Cylindrical pressure vessels are commonly used in industry to serve as tanks or boilers. The material of the cylindrical pressure vessel is subjected to a loading from all direction when it is under pressure. Stress concentration arises within a localized region of the point of load application and at sections where the member's cross sectional area changes. Specific values of stress concentration factor,  $K$ , are generally reported in graphical form in handbooks related to stress analysis. This project will provide the data necessary for stress concentration factor at two adjacent nozzles in a cylindrical pressure vessel that is very useful to designers. The stress-concentration factor associated with a specific geometry and a loading condition of a part can be derived through experimentation, analytical or computational methods.

## 1.3 Objectives and Scope of Study

The objectives of this project are:

- a) To investigate the stress distribution at two adjacent nozzles in a cylindrical pressure vessel.
- b) To determine and to plot the diagram of stress concentration factor at two adjacent nozzles in a cylindrical pressure vessel.

For this project, a computational method using finite-element technique is used as it provides a powerful and inexpensive computational method of assessing stress-concentration factors. This project covers the study within the scope of the thin-walled cylindrical pressure vessel by using relevant formulas, CATIA and ANSYS Workbench. The whole project started with the knowledge gathering and theoretical studies. Analytical techniques are involved in finding the stress concentration factor at two adjacent nozzles in a cylindrical pressure vessel. The center to center distance of the nozzles,  $L$ , normalized with the diameter of nozzles,  $d_n$ , is varied for different nozzles thickness,  $t_n$ , to nozzles radius,  $r_n$  ratios.

## CHAPTER 2

### LITERATURE REVIEW

According to Shigley, Mischke and Budynas, [3] the regions in which the state of stress is significantly greater than the theoretical predictions are as a result of:

- Geometric discontinuities or *stress raisers* such as holes, notches, and fillets;
- Internal microscopic irregularities (non-homogeneities) of the material created by such manufacturing processes as casting and molding;
- Surface irregularities such as cracks and marks created by machining operations.

These stress concentrations have highly localized effects which are the functions of geometry and loading. The stress concentration factor associated with a specific geometry and loading condition of a part, can be derived through experimentation, analytical or computational methods [4].

- **Experimental Methods.** Optical methods, such as photo elasticity, are very dependable and widely used for determining the stress concentration at a point on a part experimentally. However, several alternative methods have been used historically: the grid method, brittle-coating, brittle-model and strain gauge.
- **Analytical Methods.** The theory of elasticity can be used to analyze certain geometrical shapes to calculate stress concentration factors.
- **Computational Methods.** Finite element techniques provide a powerful and inexpensive computational method of assessing stress concentration factors.

According to Hibbeler (2005), the stress concentration factor,  $K$ , is defined as a ratio of the maximum stress to the average stress acting at the smallest cross section:

$$K = \frac{\sigma_{maximum}}{\sigma_{average}} \quad (2.1)$$

Hibbeler explains that when an axial force is applied to a member, it creates a complex stress distribution within a localized region of the point of load application. Not only do complex stress distributions arise just under a concentrated loading, they also arise at sections where the member's cross sectional area changes. Specific values of  $K$  are generally reported in graphical form in handbooks related to stress analysis. In particular, note that  $K$  is independent of the bar's material properties; rather it depends only on the bar's geometry and the type of discontinuity. As the size of  $r$  of the discontinuity is decreased, the stress concentration is increased [5].

Hibbeler also points out that when the cylindrical vessels are under pressure, the material which they are made is subjected to a loading from all directions. Since this is a 3-dimensional problem, the following formula will be used to find the stress concentration factor at two adjacent nozzles in cylindrical pressure vessel.

$$K = \frac{\sigma_{Von\ Mises\ Stress}}{\sigma_{Von\ Mises\ Stress\ without\ nozzles}} = \frac{\sigma_{max\ Von\ Mises}}{\sigma_{eff}} \quad (2.2)$$

Although this is the case, the vessel can be analyzed in a simpler manner provided it has a thin wall. In general, "thin wall" refers to a vessel having an inner-radius-to-wall-thickness ratio of 10 or more ( $r/t > 10$ ). When the vessel wall is "thin", the stress distribution throughout its thickness will not vary significantly and it is assumed that it is uniform or constant. By using this assumption, the state of stress in thin-walled cylindrical pressure vessels can be analyzed.

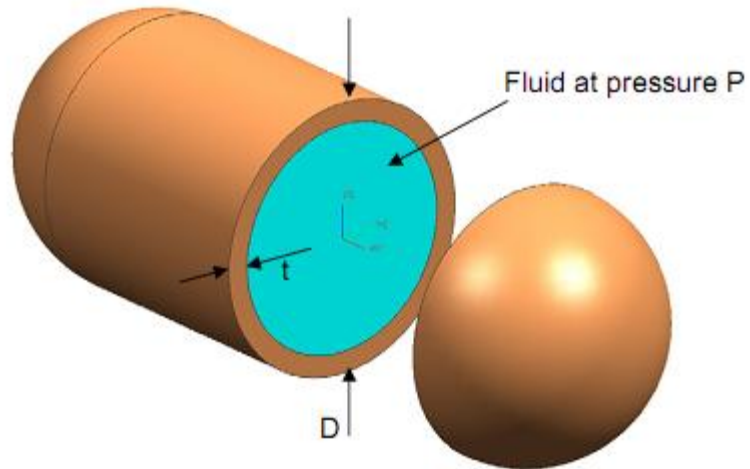


**Figure 2.1:** Cylindrical Vessel

The cylindrical pressure vessel in Figure 2.1 above has closed ends and contains fluid at gauge pressure  $P$ . The outer diameter is  $D$  and the wall thickness is  $t$ . The term ‘thin-wall’ may be taken to mean that  $D/t > 10$  [6].

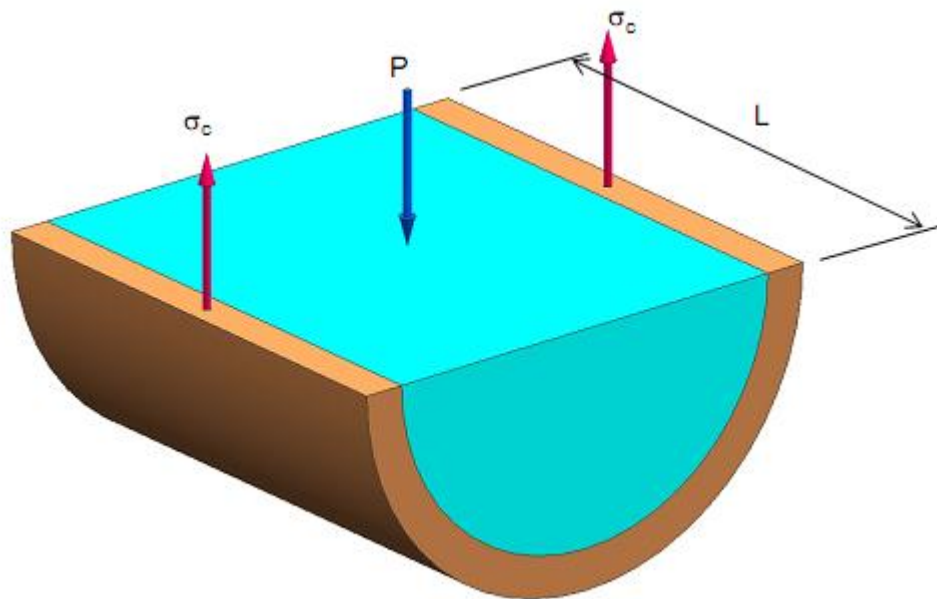


**Figure 2.2:** A free-body diagram of the back segment

If we section the cylinder, of length  $L$  and its contents across its diameter as seen above, we see that we must have equilibrium of the forces due to the internal pressure  $P$  and the circumferential stress  $\sigma_c$  in the wall. This gives

$$PLD = 2\sigma_c Lt \quad \text{where } D = 2r$$

$$\text{Or,} \quad \sigma_c = \frac{Pr}{t} \quad (2.3)$$

It is the circumferential stress in the wall. Note that we have assumed that the stress is uniform across the thickness and that we have ignored the fact that the pressure acts on an area defined by the inner diameter. These are only acceptable if  $D/t > 10$  [6].

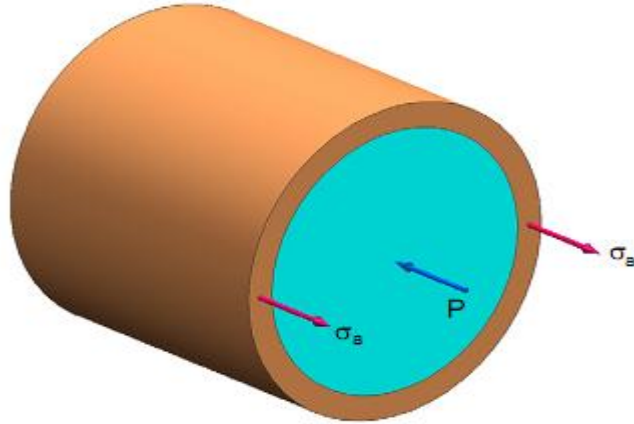


**Figure 2.3:** A free-body diagram to find the longitudinal stress

If the cylinder has closed ends, the axial stress  $\sigma_a$  in the wall is found in a similar way by considering a transverse section as shown in Figure 2.3 above. Equilibrium of forces gives:

$$P\pi r^2 = \sigma_a \pi D t \quad \text{where } D = 2r$$

and thus the axial stress,

$$\sigma_a = \frac{Pr}{2t} \quad (2.4)$$

The same assumptions apply. Note that  $\sigma_c$  and  $\sigma_a$  are principal stresses and remember that the third principal stress  $\sigma_3 = 0$ . The maximum shear stress is thus

$$\tau_{\max} = \frac{|\sigma_1 - \sigma_3|}{2} = \frac{Pr}{2t} \quad (2.5)$$

By comparing equations (2.3) and (2.4), the circumferential stress is twice as large as the longitudinal stress.

The distortion-energy theory states that yielding begins whenever the distortion energy in a unit volume equals the distortion energy in the same volume when uniaxially stressed to the yield strength. The effective stress or Von Mises Stress for a biaxial stress state becomes:

$$\sigma_{\text{eff}} = \sqrt{\sigma_1^2 - \sigma_1 \sigma_2 + \sigma_2^2} \quad (2.6)$$

# CHAPTER 3

## METHODOLOGY

In order to achieve the objectives of the project, research and analysis are done on stress concentration factor at two adjacent nozzles in a cylindrical pressure vessel.

### 3.1 Process Plan

The flow chart in Figure 3.1 below shows the main activities of this project.

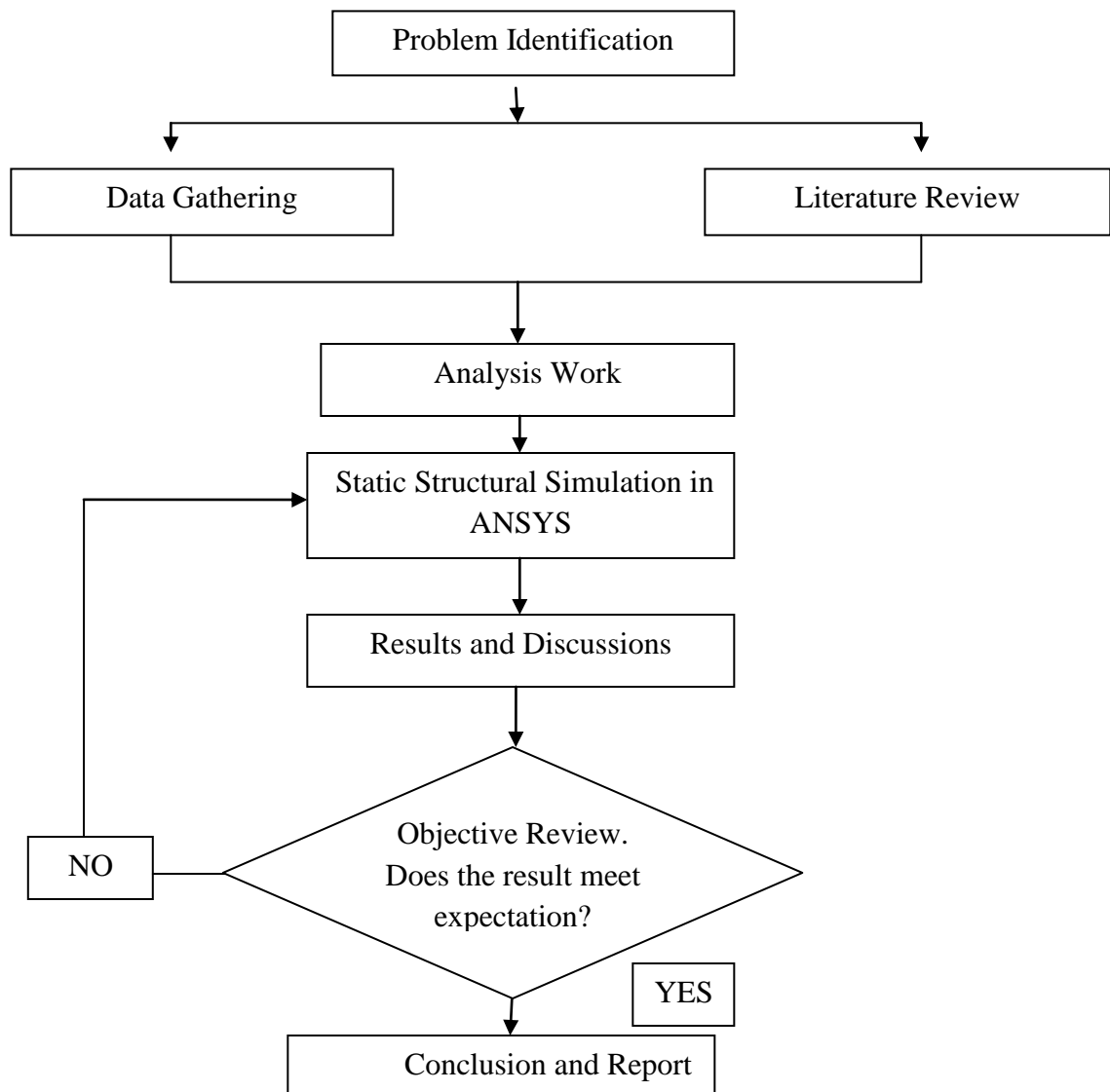


Figure 3.1: Project Flow

### 3.2 Data Gathering

For the first case, center to center distance of the nozzles,  $L$ , over diameter of the nozzle,  $d_n$ , ( $L / d_n$ ), diameter of the nozzles is kept constant at 40 mm and the length of the pressure vessel,  $l$  is fixed at 544mm. For the second case, which is the nozzles radius,  $r_n$  over nozzles thickness,  $t_n$ , ( $r_n / t_n$ ), the nozzles radius is held constant at 20 mm. Below are the dimensions of the other parameters:

- a) Thickness of the pressure vessel,  $t_c = 10\text{mm}$
- b) Radius of the pressure vessel,  $r_c = 500\text{mm}$
- c) Nozzles height,  $h = 150\text{mm}$
- d) The vessel is subjected to a pressure,  $p = 10\text{ bar}$

The properties of the structural steel are as in Table 3.1

**Table 3.1:** Properties of Structural Steel

Structural Properties	
Young's Modulus	200 GPa
Poisson's Ratio	0.3
Density	7850. kg/m <sup>3</sup>
Tensile Yield Strength	250 MPa
Compressive Yield Strength	250 MPa
Tensile Ultimate Strength	460 MPa
Compressive Ultimate Strength	Not available

### 3.3 Finite Element Model

Finite element analyses of the vessel are performed by using ANSYS Workbench. Before the models are being analyzed in ANSYS, the models are generated in CATIA.

For this project, there will be 5 types of nozzle placement where the stress at the nozzles will be studied. Figure 3.2 to 3.6 show the condition of the nozzles.

- a) Nozzles in longitudinal direction (Figure 3.2)

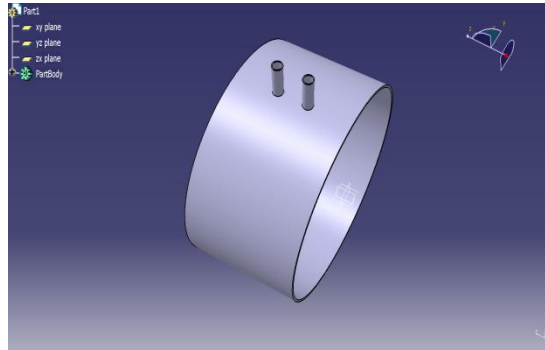


**Figure 3.2:** Model Generated in CATIA with nozzles in longitudinal direction

- b) Nozzles in circumferential direction (Figure 3.3)

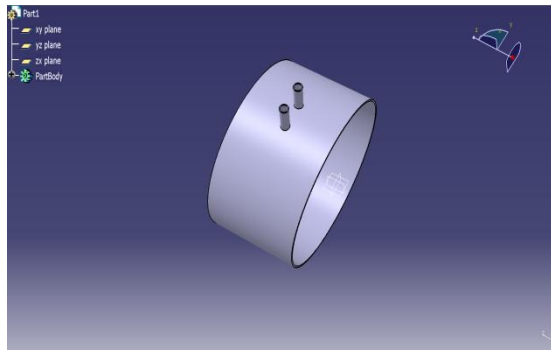


**Figure 3.3:** Model Generated in CATIA with nozzles in circumferential direction

c) Nozzles  $30^{\circ}$  from one another (Figure 3.4)

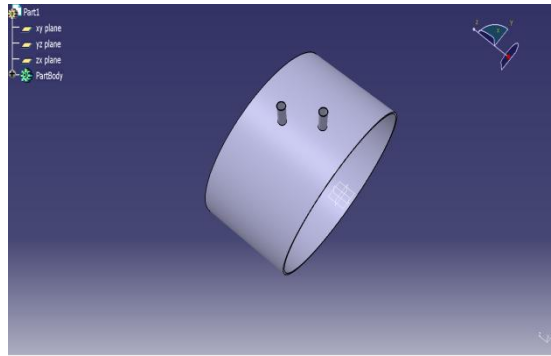


**Figure 3.4:** Generated in CATIA with nozzles  $30^{\circ}$  from one another

e) Nozzles  $45^{\circ}$  from one another (Figure 3.5)

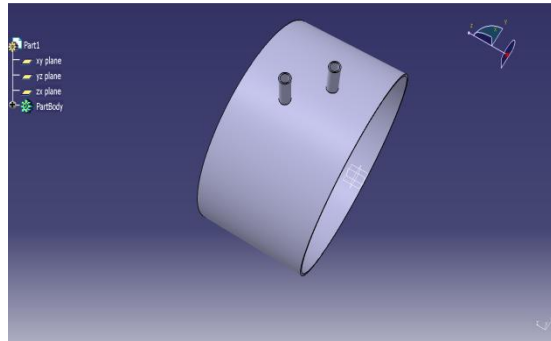


**Figure 3.5:** Generated in CATIA with nozzles  $45^{\circ}$  from one another

e) Nozzles  $60^{\circ}$  from one another (Figure 3.6)

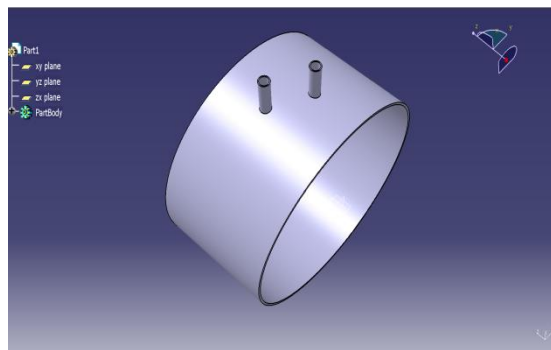


**Figure 3.6:** Generated in CATIA with nozzles  $60^{\circ}$  from one another

### **3.4 Loading Conditions**

There are three loadings imposed to the model. The first loading is the pressure that is imposed to the inner surface of the pressure vessel and the nozzles. The second and third loadings are the stresses that are imposed in the axial direction of the pressure vessel and at the end of nozzles faces.

### **3.5 Software Required**

The software required for this project are CATIA and ANSYS Workbench. Besides that, other software that will be used is Microsoft Office 2007 for documentation purpose. ANSYS is a comprehensive general-purpose finite element computer program that contains over 100000 lines of codes. ANSYS is capable of performing static, dynamic, heat transfer, fluid flow and electromagnetism analysis.

### 3.6 Key Milestones

The key milestones for Final Year Project 2 is shown in Table 3.2

**Table 3.2:** Key Milestones for Final Year Project 2

Date	FYP 2
20 <sup>th</sup> August 2010	Progress Report 1
20-24 <sup>th</sup> September 2010	Progress Report 2 and Seminar
11 <sup>st</sup> October 2010	Poster Submission
1 <sup>st</sup> November 2010	Dissertation Draft
8-12 <sup>nd</sup> November 2010	Oral Presentation
7 days after oral	Hardbound Dissertation

### 3.7 Gantt Chart

The Gantt chart for Final Year Project 2 is shown in Figure 3.7

No	Detail/Week	1	2	3	4	5	6	7	8	9	10	11	12	13	14
1	Project Work Continues	█	█	█											
2	Submission of Progress Report I				█										
3	Project Work Continues			█	█	█	█								
4	Submission of Progress Report II								█						
5	Seminar								█	█					
6	Project Work Continues							█	█	█	█	█	█	█	█
7	Poster Exhibition											█			
8	Submission of Dissertation Final Draft														█
9	Oral Presentation											Study Week			
10	Submission of Dissertation								7 days after oral presentation						

**Figure 3.7:** Gantt chart for Final Year Project 2

## CHAPTER 4

### RESULTS AND DISCUSSIONS

In order to investigate and to plot the diagram of stress concentration factor,  $K$ , at two longitudinal adjacent nozzles in a cylindrical pressure vessel the following parameters are varied:

- a) Center to center distance of the nozzles,  $L$ , over the diameter of the nozzle,  $d_n$ , ( $L/d_n$ ).
- b) Nozzle thickness,  $t_n$ , over the nozzle radius,  $r_n$ , ( $r_n/t_n$ )

#### 4.1 Analytical Findings

The analytical findings for center to center distance of the nozzles,  $L$ , over diameter of the nozzles,  $d_n$ , ( $L/d_n$ ) and the nozzles thickness,  $t_n$ , over nozzles radius,  $r_n$ , ( $r_n/t_n$ ) are shown in Table 4.1 and Table 4.2.

**Table 4.1:** Analytical Findings ( $L/d_n$ )

$L/d_n$	Center to center distance, $L$ (mm)
<b>2.0</b>	80
<b>2.5</b>	100
<b>3.0</b>	120
<b>3.5</b>	140
<b>4.0</b>	160
<b>4.5</b>	180
<b>5.0</b>	200

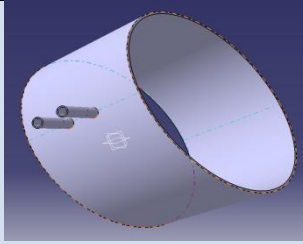
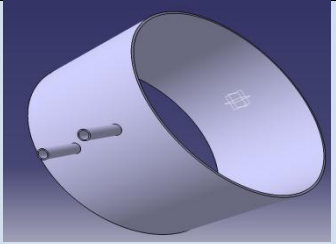
**Table 4.2:** Analytical Findings ( $r_n/t_n$ )

$r_n/t_n$	Nozzle thickness
<b>4.0</b>	5.0
<b>5.0</b>	4.0
<b>10.0</b>	2.0

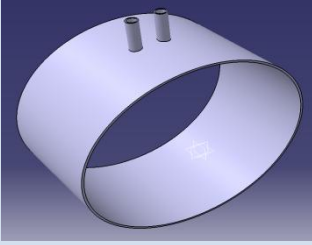
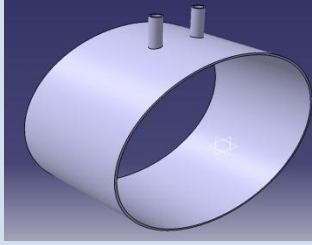
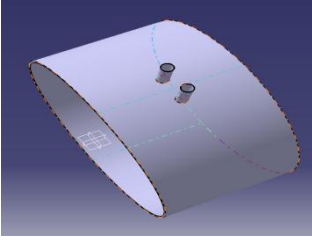
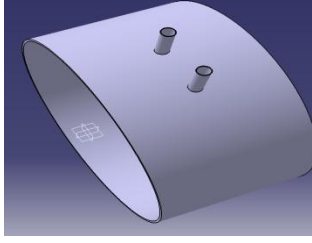
## 4.2 Model Generation

Table 4.3 to 4.7 shows the example of models that are generated in CATIA before they are imported into ANSYS for meshing and simulation.

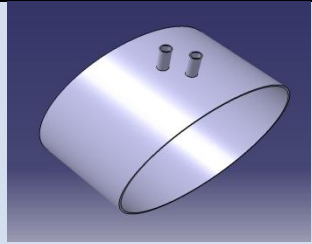
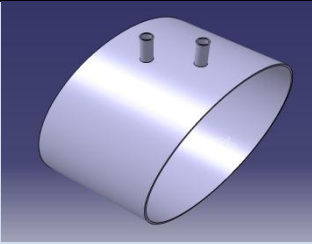
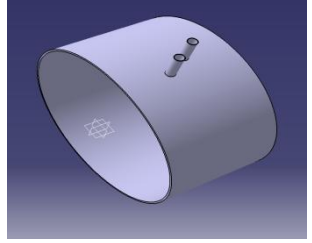
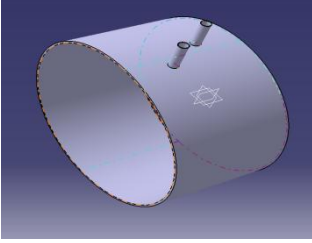
**Table 4.3:** Models generation for nozzles in longitudinal direction

	$L/d_n=3$	$L/d_n=5$
$r_n/t_n=4$		
$r_n/t_n=10$		

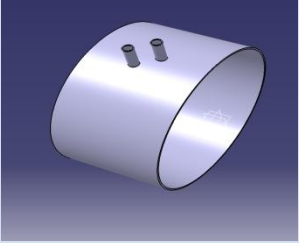
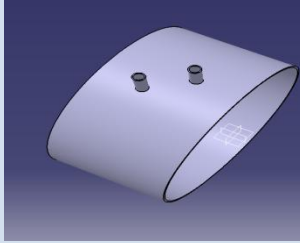
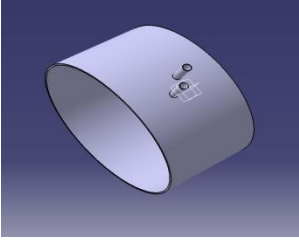
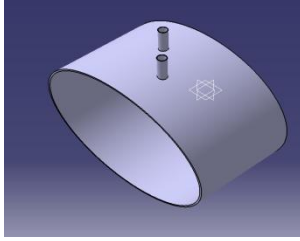
**Table 4.4:** Models generation for nozzles in circumferential direction

	$L/d_n=3$	$L/d_n=5$
$r_n/t_n=4$		
$r_n/t_n=10$		

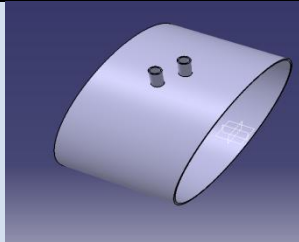
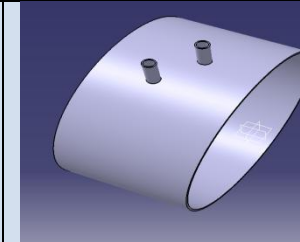
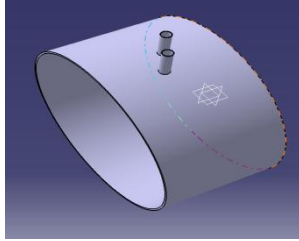
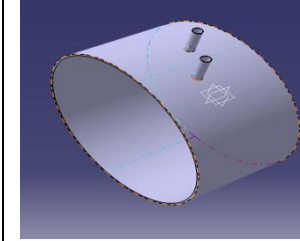
**Table 4.5:** Models generation for nozzles  $30^\circ$  from one another

	$L/d_n=3$	$L/d_n=5$
$r_n/t_n=4$		
$r_n/t_n=10$		

**Table 4.6:** Models generation for nozzles  $45^\circ$  from one another

	$L/d_n=3$	$L/d_n=5$
$r_n/t_n=4$		
$r_n/t_n=10$		

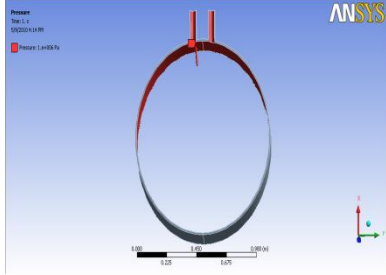
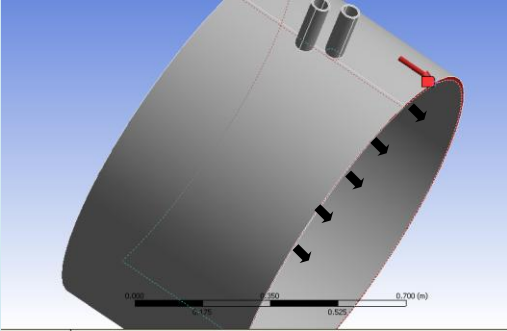
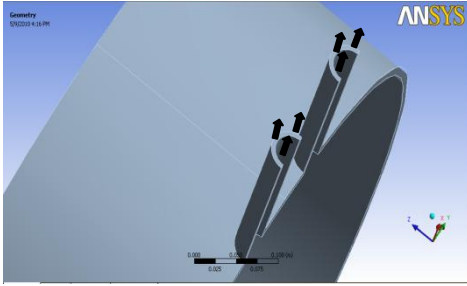
**Table 4.7:** Models generation for nozzles  $60^\circ$  from one another

	$L/d_n=3$	$L/d_n=5$
$r_n/t_n=4$		
$r_n/t_n=10$		

### 4.3 Loading

The loadings that are imposed to the model are shown in Table 4.8

**Table 4.8:** Loading imposed to the model

<p style="text-align: center;"><b>Loading(inner surface)</b></p> 	<p>At every surface of shaded area(normal to the pressure vessel and nozzles) Pressure, <math>P = 10 \text{ bar} = 1 \text{ MPa}</math>.</p>
<p style="text-align: center;"><b>Loading(right side)</b></p> 	$\sigma_2 = \frac{Pr_c}{2t_c}, p = 1 \text{ MPa}$ $\sigma_2 = \frac{(1 \text{ MPa})(500 \text{ mm})}{(2)(10 \text{ mm})}$ $= 25 \text{ MPa}$
<p style="text-align: center;"><b>Loading for nozzles</b></p> 	$\sigma = \frac{Pr_n}{2t_n}$ <p>For <math>r_n/t_n = 10</math></p> $\sigma = \frac{(1 \text{ MPa})(20 \text{ mm})}{(2)(2 \text{ mm})}$ $= 5 \text{ MPa}$ <p>For <math>r_n/t_n = 5</math>; <math>\sigma = 2.5 \text{ MPa}</math> For <math>r_n/t_n = 4</math>; <math>\sigma = 2.0 \text{ MPa}</math></p>

#### 4.4 Meshing

Meshing is done by using hex dominant technique and face sizing control. A sample of FEA model is shown in Figure 4.1. This is the example for the parameter  $r_i/t_n = 4$  and  $L/d_n = 2$ . For this case, the number of elements generated is 10004 and the number of nodes is 49791.

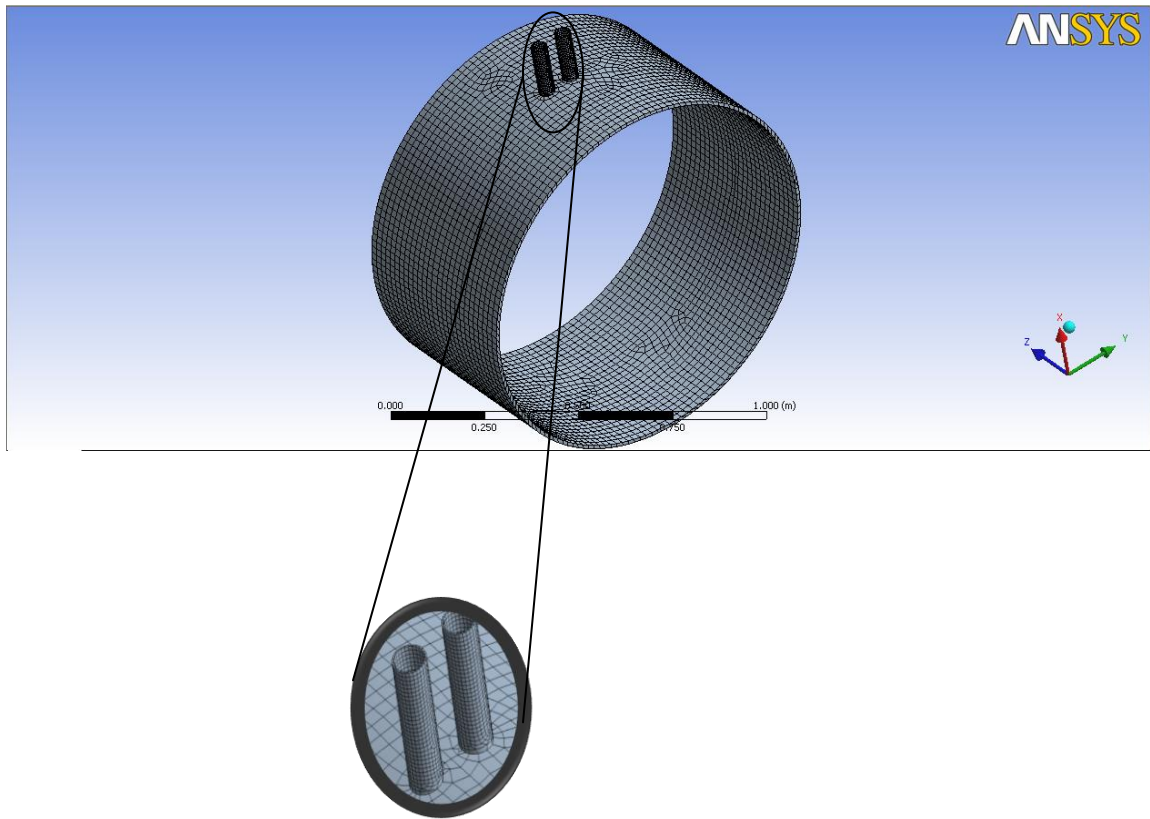


**Figure 4.1:** Sample of FEA Model

## 4.5 Results and Discussions

### 4.5.1 Results for nozzles in longitudinal direction

This is the result for the condition where the nozzles are in longitudinal direction.

Table 4.9 and Figure 4.2 shows the result for  $r_n/t_n = 4$ .

**Table 4.9:** Results for nozzles in longitudinal direction for  $r_n/t_n = 4$

$L/d_n$	Average Stress (MPa)	Maximum Stress ( MPa)	Stress Concentration Factor, K
2.0	43.301	139.13	3.2131
2.5	43.301	132.68	3.0641
3.0	43.301	131.71	3.0417
3.5	43.301	126.79	2.9281
4.0	43.301	128.55	2.9688
4.5	43.301	126.21	2.9147
5.0	43.301	126.07	2.9114

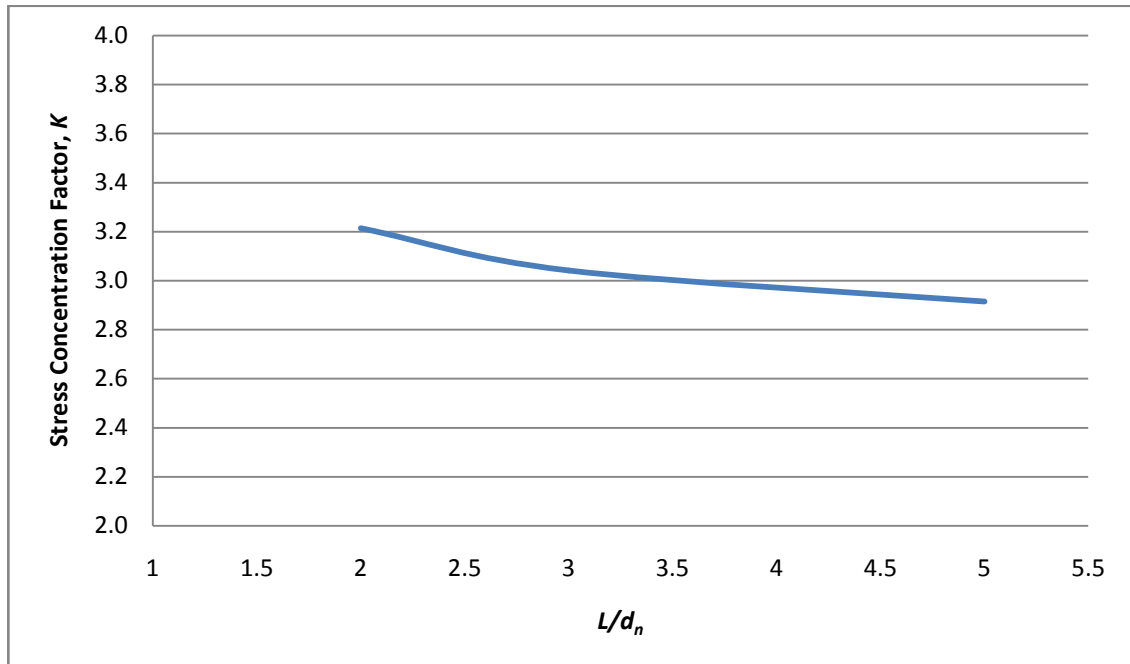


**Figure 4.2:** Stress Concentration Factor, K vs  $L/d_n$  for  $r_n/t_n = 4$

Table 4.10 and Figure 4.3 shows the result for  $r_n/t_n = 5$ .

**Table 4.10:** Results for nozzles in longitudinal direction for  $r_n/t_n = 5$

$L/d_n$	Average Stress (MPa)	Maximum Stress ( MPa)	Stress Concentration Factor, K
2.0	43.301	141.32	3.2637
2.5	43.301	134.59	3.1082
3.0	43.301	129.55	2.9918
3.5	43.301	128.48	2.9671
4.0	43.301	126.43	2.9198
4.5	43.301	128.40	2.9652
5.0	43.301	127.49	2.9443

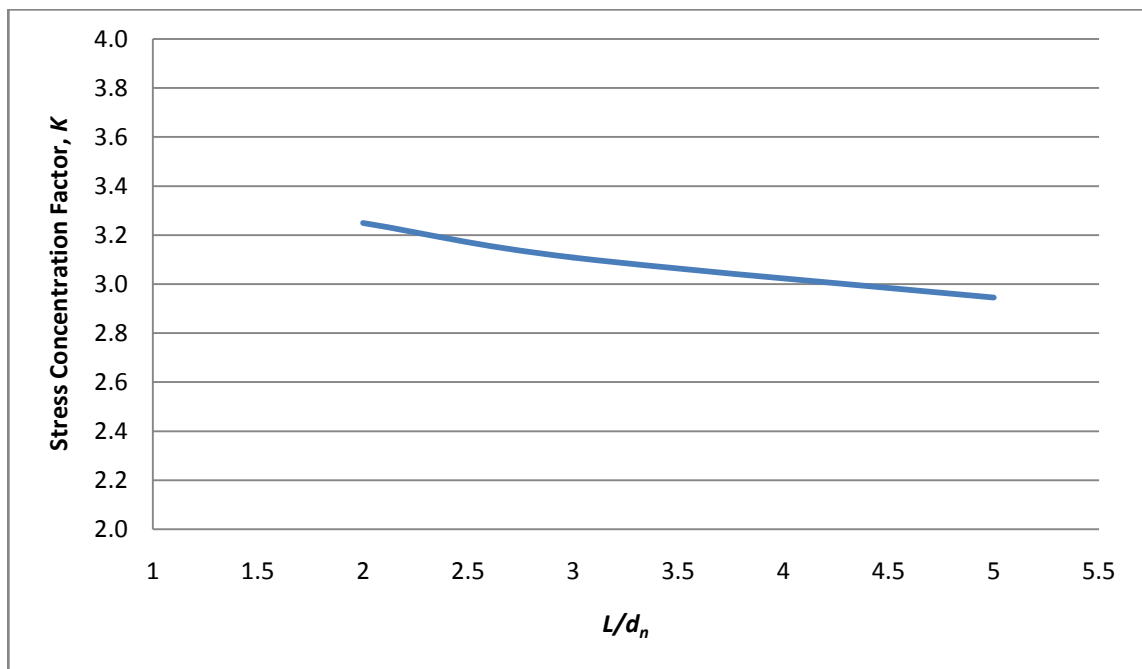
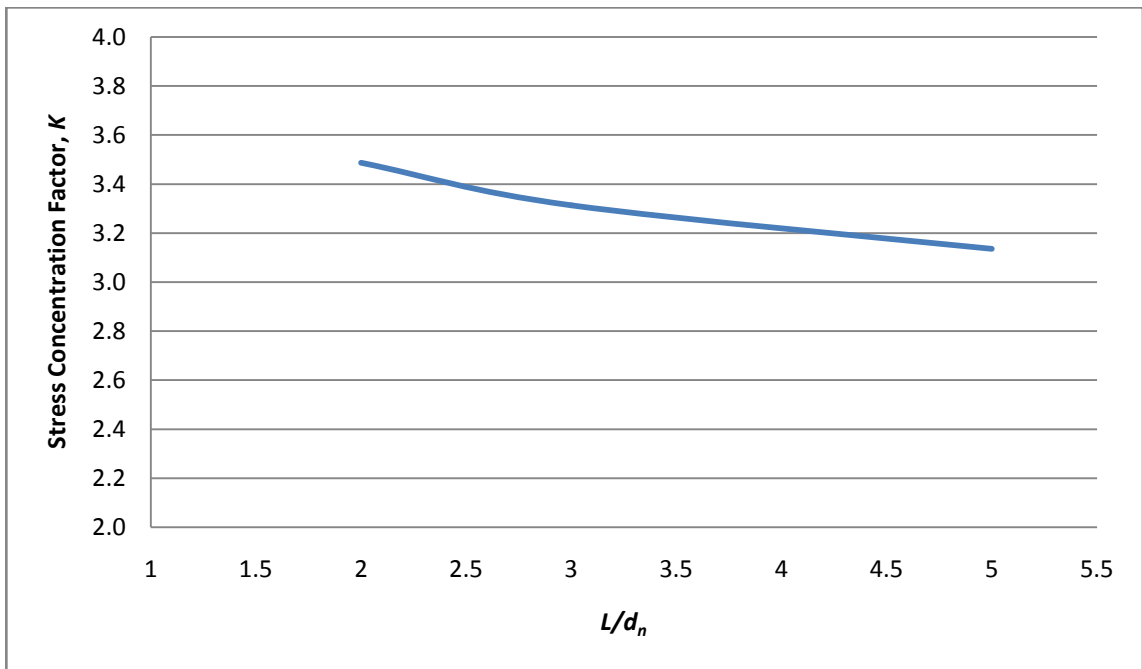


**Figure 4.3:** Stress Concentration Factor,  $K$  vs  $L/d_n$  for  $r_n/t_n = 5$

Table 4.11 and Figure 4.4 shows the result for  $r_n/t_n = 10$ .

**Table 4.11:** Results for nozzles in longitudinal direction for  $r_n/t_n = 10$

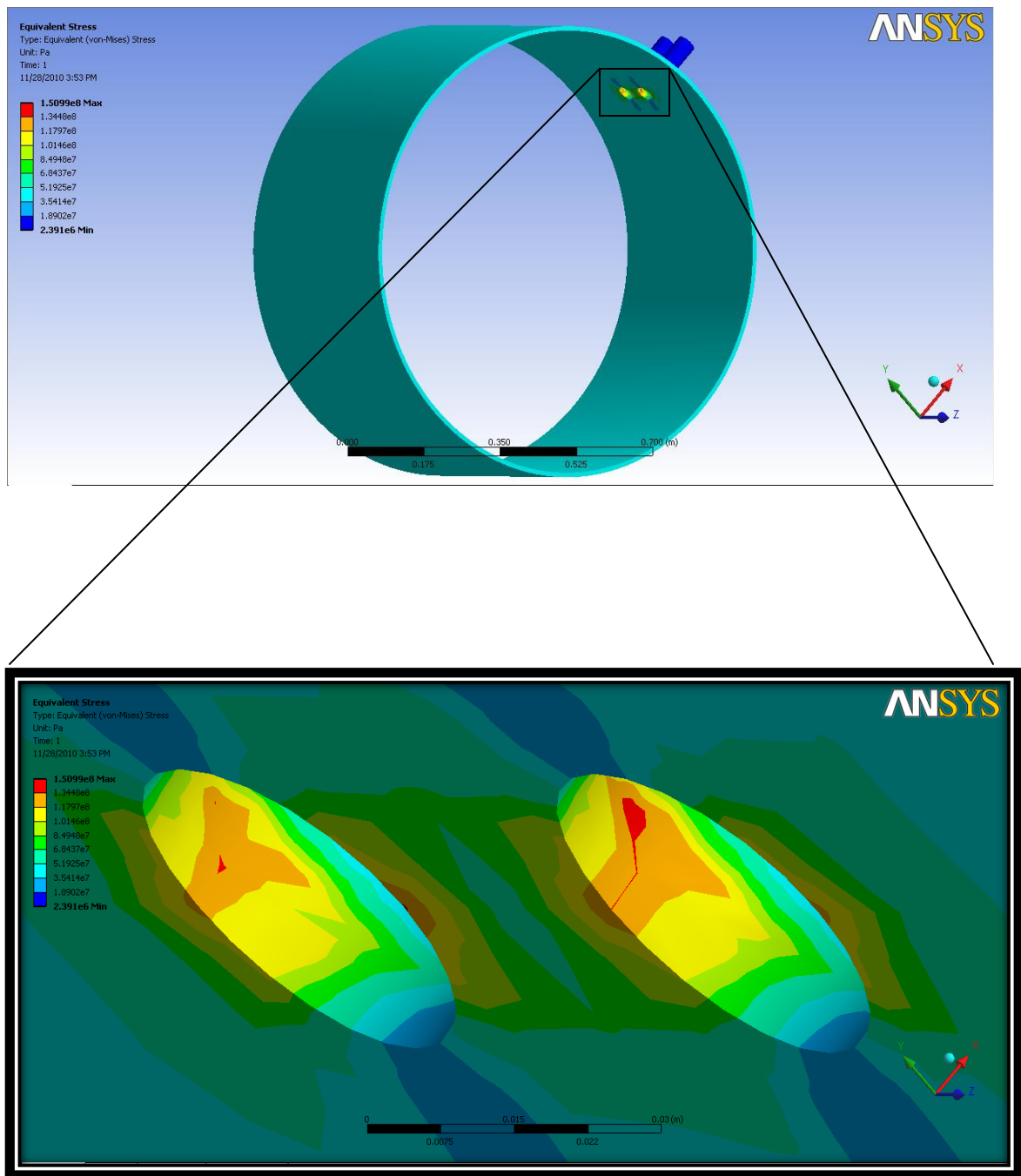
$L/d_n$	Average Stress (MPa)	Maximum Stress ( MPa)	Stress Concentration Factor, K
2.0	43.301	150.99	3.4870
2.5	43.301	148.07	3.4196
3.0	43.301	143.46	3.3131
3.5	43.301	140.86	3.2530
4.0	43.301	136.78	3.1589
4.5	43.301	136.82	3.1597
5.0	43.301	135.76	3.1353



**Figure 4.4:** Stress Concentration Factor,  $K$  vs  $L/d_n$  for  $r_n/t_n = 10$

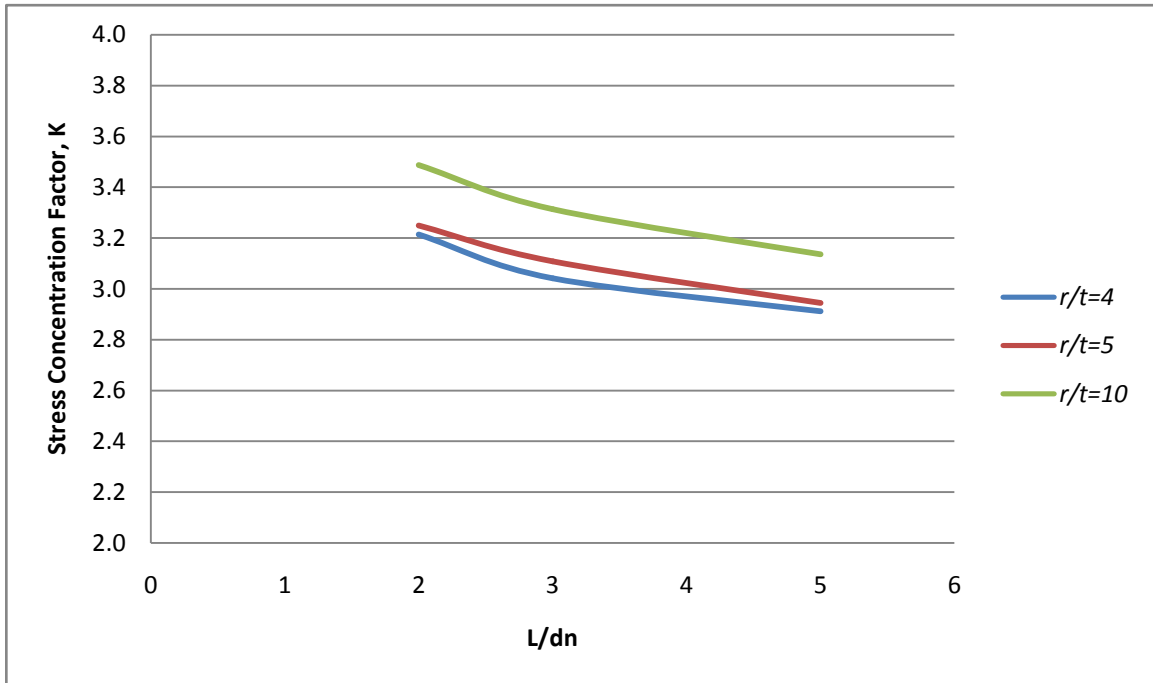
From simulation, the maximum stress occurred at the junction of nozzles-vessel.

Figure 4.5 shows a sample of ANSYS simulation for nozzles in longitudinal direction.



**Figure 4.5:** Samples of ANSYS simulation for nozzles in longitudinal direction

Figure 4.6 below shows the overall result for nozzles in longitudinal direction.



**Figure 4.6:** Stress Concentration Factor,  $K$  vs  $L/d_n$  for nozzles in longitudinal direction

The rest of the simulation results for nozzles in longitudinal direction are attached in the Appendices. In short, the maximum stress occurs at the junction of pressure vessel-nozzles because the state of stress there is significantly greater due to the geometric discontinuities caused by the holes. The value of stress concentration factor,  $K$  will decrease as the result of increasing the center to center distance,  $L$  between the two nozzles. It also decreases with the increase of the thickness of the nozzles,  $t_n$ .

#### 4.5.2 Results for nozzles in circumferential direction

This is the result for the condition where the nozzles are in circumferential direction. Table 4.12 and Figure 4.7 shows the result for  $r_n/t_n = 4$ .

**Table 4.12:** Results for nozzle in circumferential direction for  $r_n/t_n = 4$

$L/d_n$	Average Stress (MPa)	Maximum Stress ( MPa)	Stress Concentration Factor, K
2.0	43.301	140.89	3.2537
2.5	43.301	139.18	3.2142
3.0	43.301	134.75	3.1119
3.5	43.301	131.88	3.0457
4.0	43.301	127.38	2.9417
4.5	43.301	123.97	2.8630
5.0	43.301	122.30	2.8244

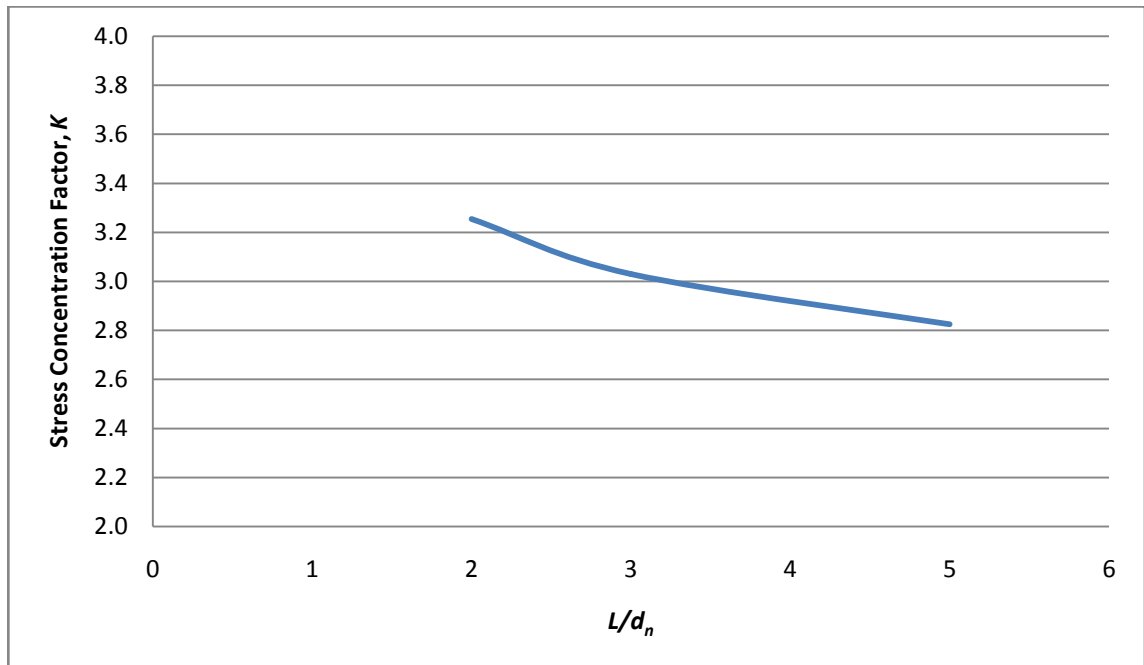


**Figure 4.7:** Stress Concentration Factor,  $K$  vs  $L/d_n$  for  $r_n/t_n = 4$

Table 4.13 and Figure 4.8 shows the result for  $r_n/t_n = 5$ .

**Table 4.13:** Results for nozzle in circumferential direction for  $r_n/t_n = 5$

$L/d_n$	Average Stress (MPa)	Maximum Stress ( MPa)	Stress Concentration Factor, K
2.0	43.301	142.28	3.2858
2.5	43.301	140.74	3.2503
3.0	43.301	136.45	3.1512
3.5	43.301	136.75	3.1581
4.0	43.301	131.98	3.0480
4.5	43.301	124.40	2.8730
5.0	43.301	123.20	2.8452

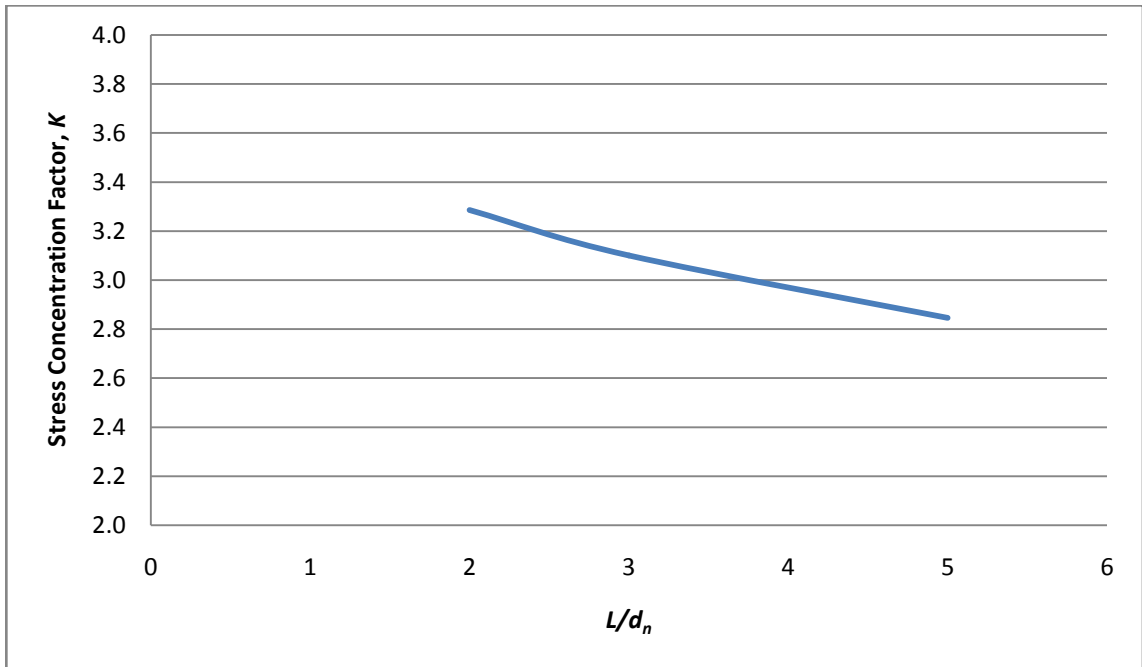
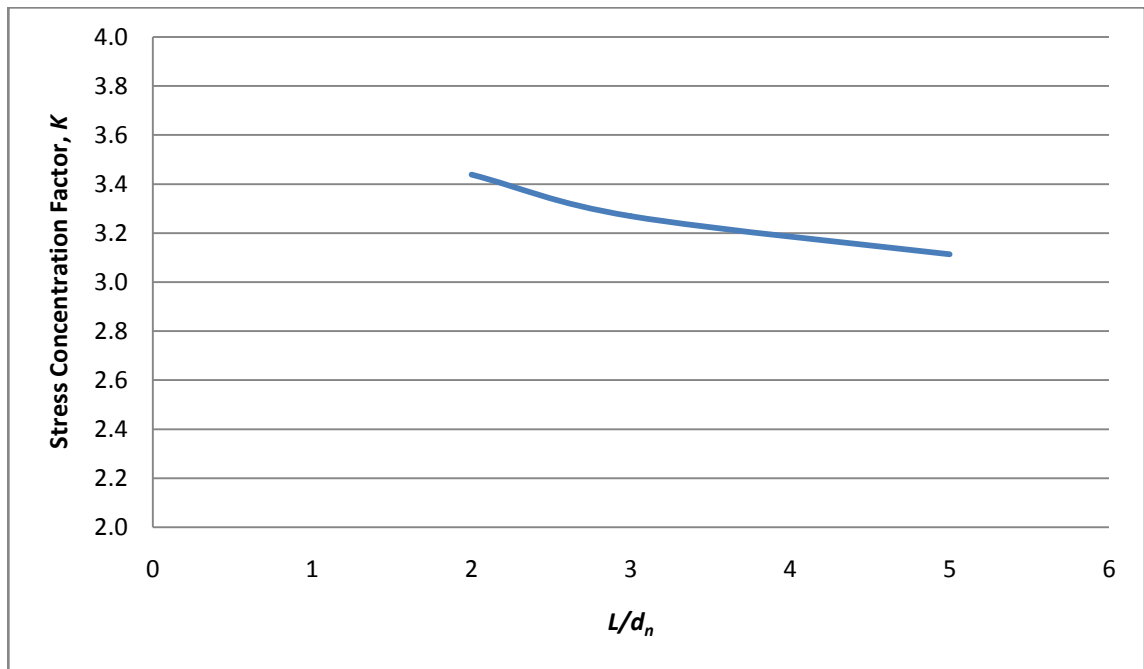


**Figure 4.8:** Stress Concentration Factor,  $K$  vs  $L/d_n$  for  $r_n/t_n = 5$

Table 4.14 and Figure 4.9 shows the result for  $r_n/t_n = 10$ .

**Table 4.14:** Results for nozzle in circumferential direction for  $r_n/t_n = 10$

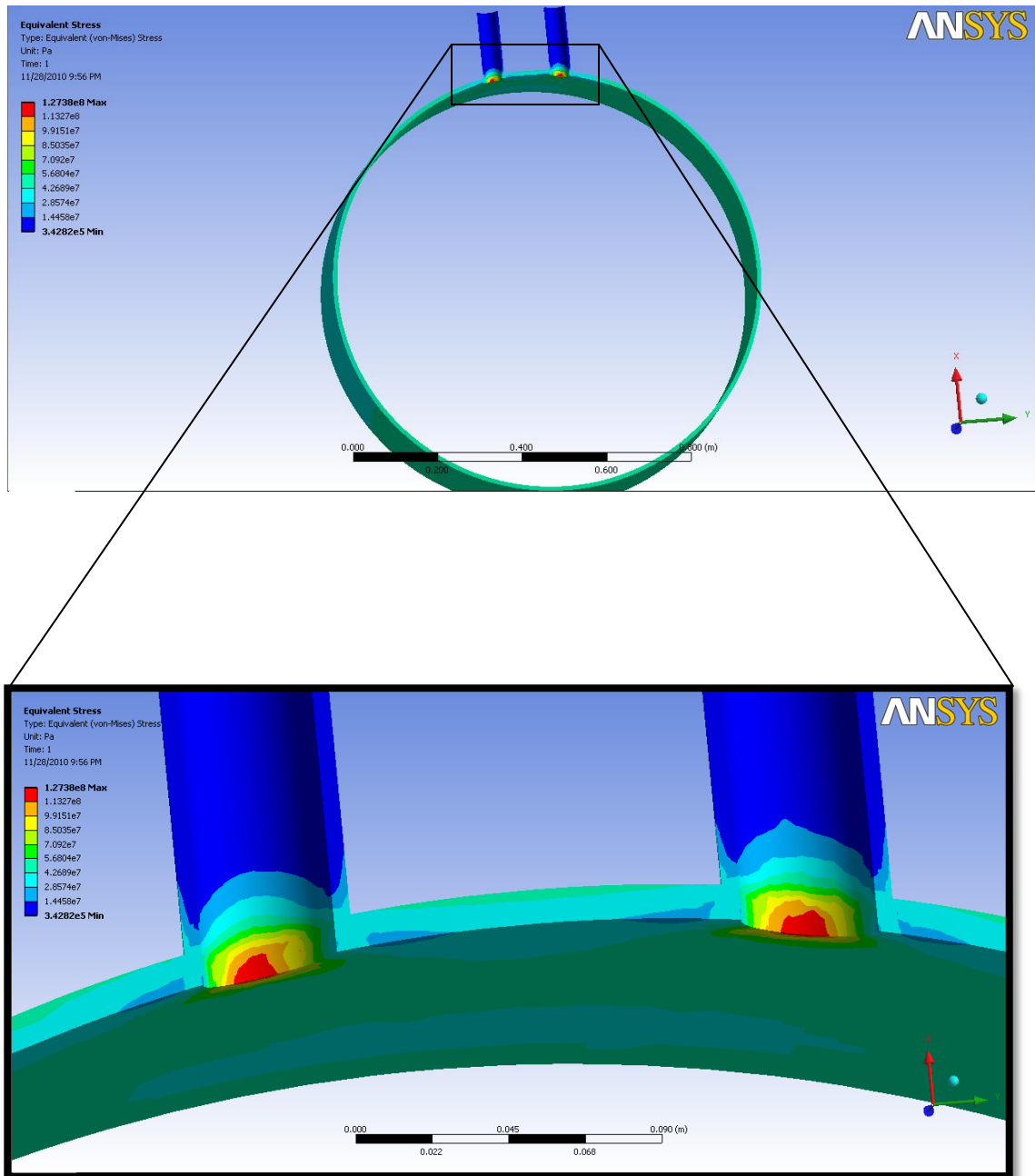
$L/d_n$	Average Stress (MPa)	Maximum Stress ( MPa)	Stress Concentration Factor, K
2.0	43.301	148.85	3.4376
2.5	43.301	141.95	3.2782
3.0	43.301	141.52	3.2683
3.5	43.301	139.16	3.2138
4.0	43.301	139.00	3.2101
4.5	43.301	138.85	3.2066
5.0	43.301	134.80	3.1131



**Figure 4.9:** Stress Concentration Factor,  $K$  vs  $L/d_n$  for  $r_n/t_n = 10$

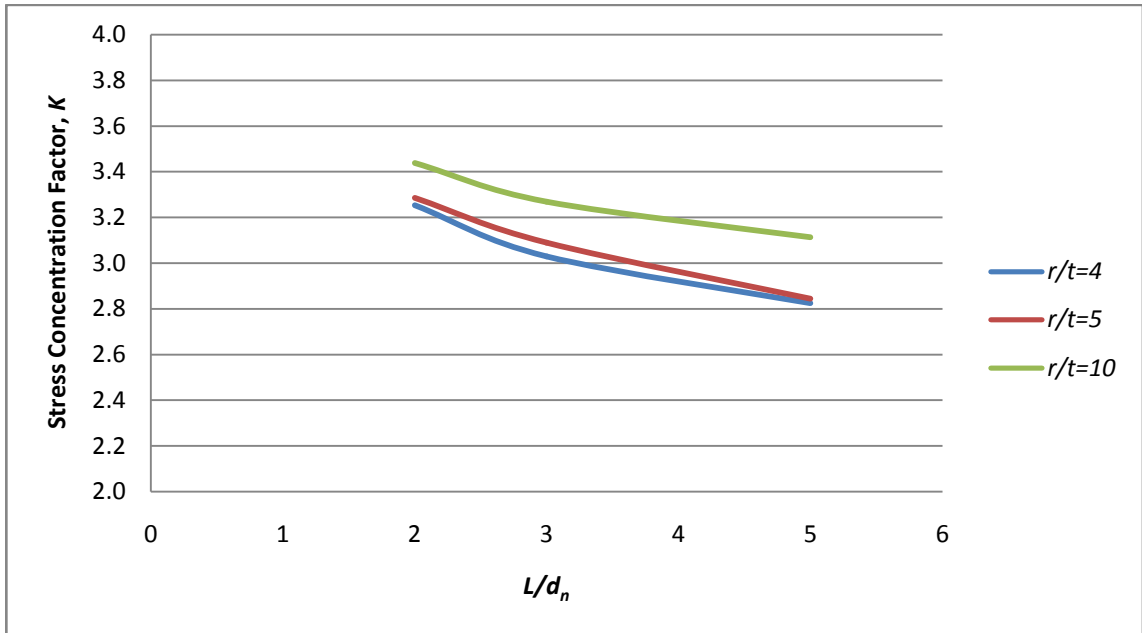
From simulation, the maximum stress occurred at the junction of nozzles-vessel.

Figure 4.10 shows a sample of ANSYS simulation for nozzles in circumferential direction.



**Figure 4.10:** Samples of ANSYS simulation for nozzles in circumferential direction

Figure 4.11 below shows the overall result for nozzles in circumferential direction.



**Figure 4.11:** Stress Concentration Factor,  $K$  vs  $L/d_n$  for nozzles in circumferential direction

The rest of the simulation results for nozzles in circumferential direction are attached in the Appendices. In short, the maximum stress occurs at the junction of pressure vessel-nozzles because the state of stress there is significantly greater due to the geometric discontinuities caused by the holes. The value of stress concentration factor,  $K$  will decrease as the result of increasing the center to center distance,  $L$  between the two nozzles. It also decreases with the increase of the thickness of the nozzles,  $t_n$ .

### 4.5.3 Results for nozzles 30° from one another.

This is the result for the condition where the nozzles are 30° from one another.

Table 4.15 and Figure 4.12 shows the result for  $r_n/t_n = 4$ .

**Table 4.15:** Results for nozzles 30° from one another for  $r_n/t_n = 4$

$L/d_n$	Average Stress (MPa)	Maximum Stress ( MPa)	Stress Concentration Factor, K
2.0	43.301	153.67	3.5489
2.5	43.301	152.85	3.5299
3.0	43.301	141.87	3.2764
3.5	43.301	139.82	3.2290
4.0	43.301	137.16	3.1676
4.5	43.301	141.89	3.2768
5.0	43.301	139.41	3.2195

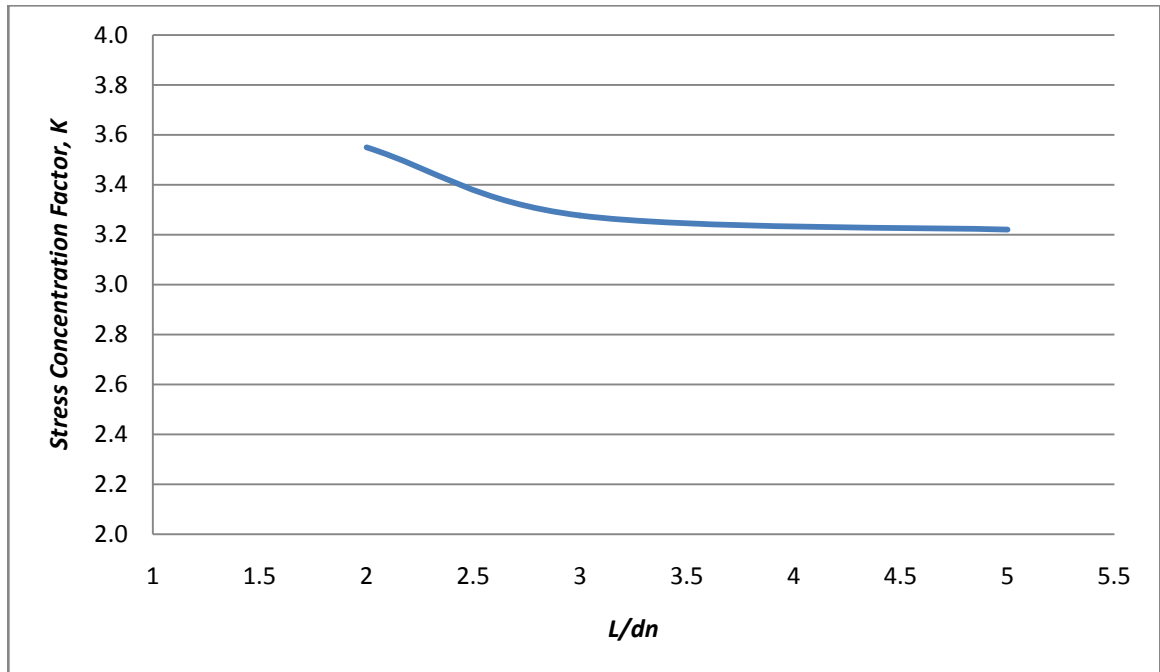


**Figure 4.12:** Stress Concentration Factor, K vs  $L/d_n$  for  $r_n/t_n = 4$

Table 4.16 and Figure 4.13 shows the result for  $r_n/t_n = 5$ .

**Table 4.16:** Results for nozzles  $30^\circ$  from one another for  $r_n/t_n = 5$

$L/d_n$	Average Stress (MPa)	Maximum Stress ( MPa)	Stress Concentration Factor, K
2.0	43.301	154.98	3.5791
2.5	43.301	153.71	3.5498
3.0	43.301	142.65	3.2944
3.5	43.301	141.12	3.2590
4.0	43.301	136.20	3.1454
4.5	43.301	140.81	3.2518
5.0	43.301	140.03	3.2339

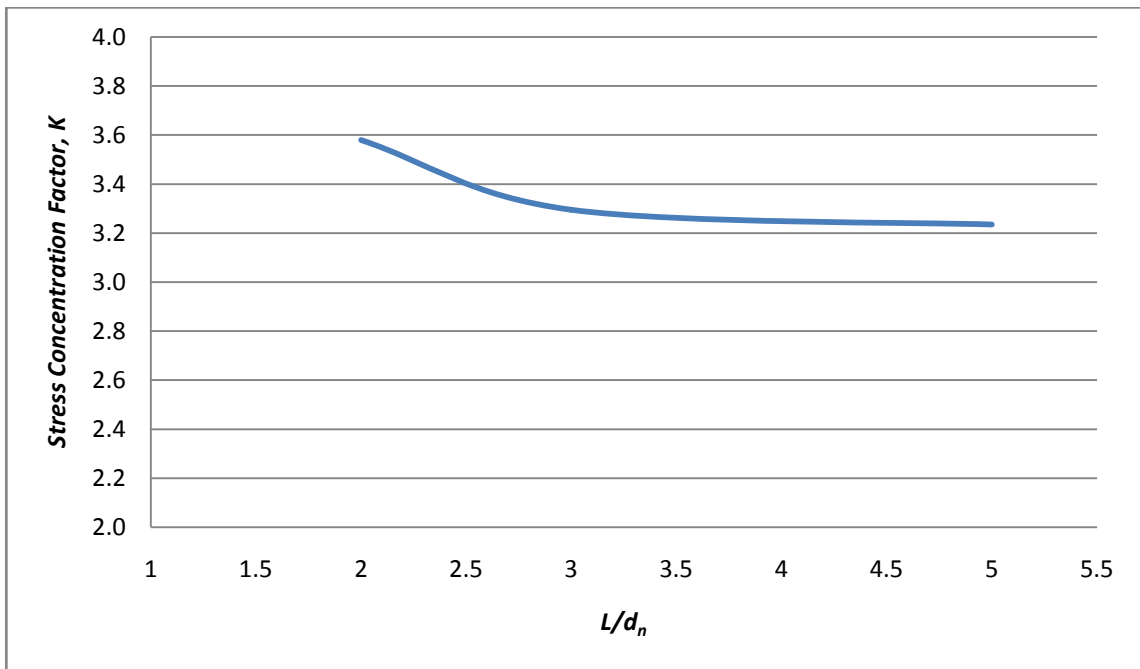
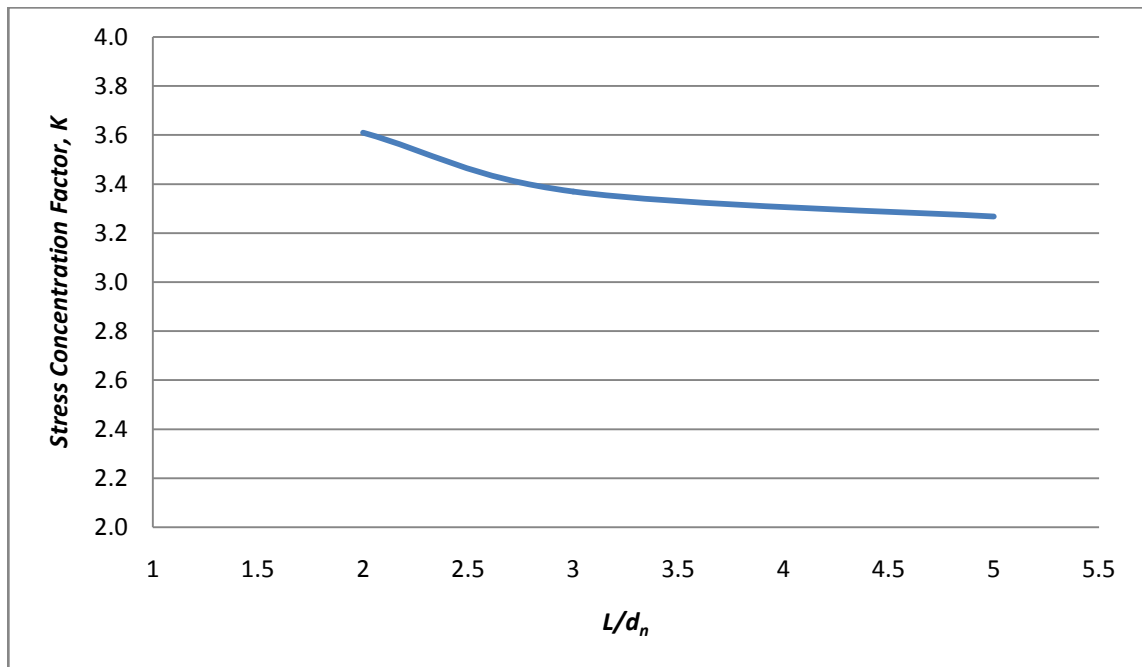


**Figure 4.13:** Stress Concentration Factor,  $K$  vs  $L/d_n$  for  $r_n/t_n = 5$

Table 4.17 and Figure 4.14 shows the result for  $r_n/t_n = 10$ .

**Table 4.17:** Results for nozzles  $30^\circ$  from one another for  $r_n/t_n = 10$

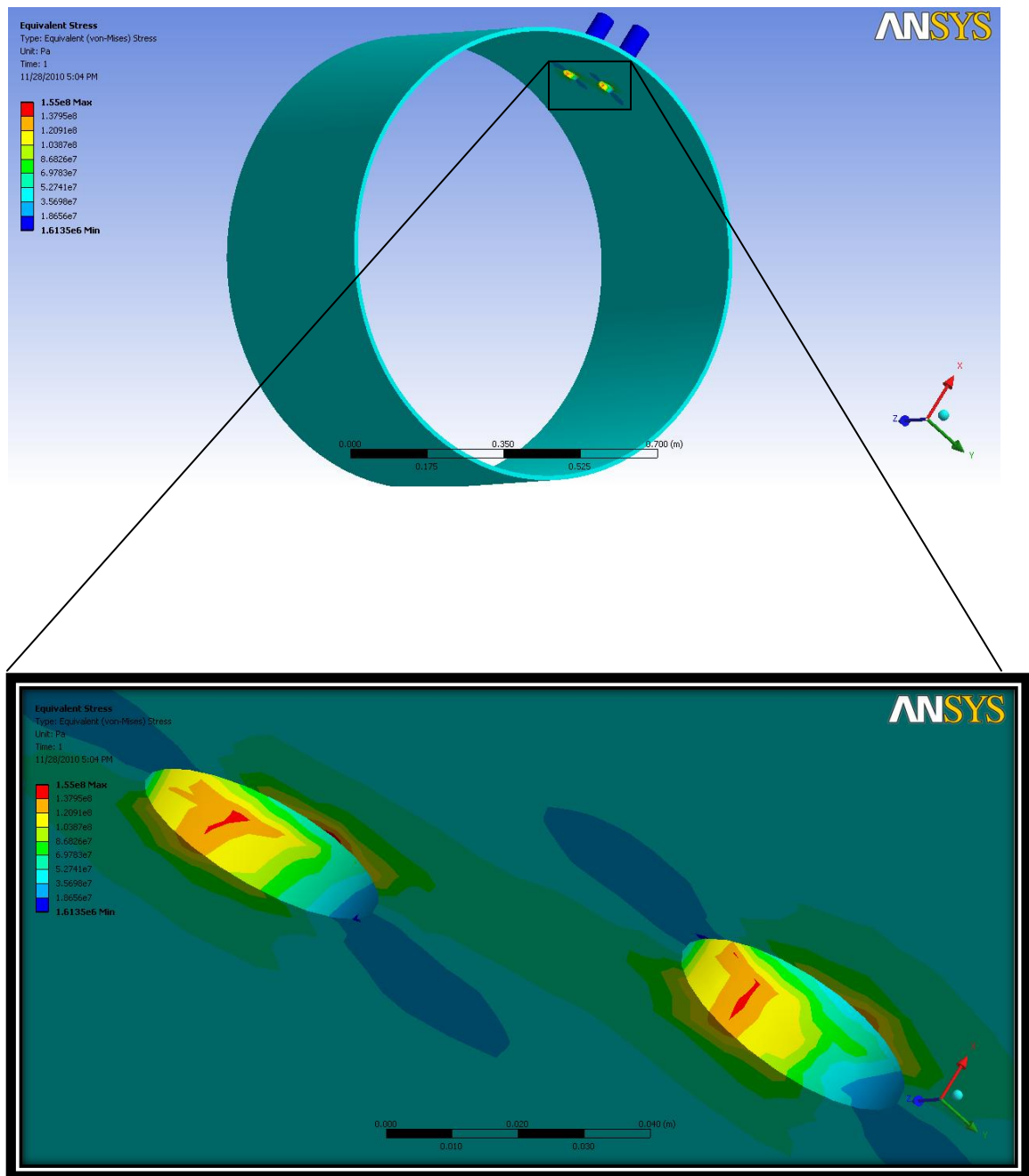
$L/d_n$	Average Stress (MPa)	Maximum Stress ( MPa)	Stress Concentration Factor, K
2.0	43.301	156.25	3.6085
2.5	43.301	155.00	3.5796
3.0	43.301	145.85	3.3683
3.5	43.301	142.73	3.2962
4.0	43.301	142.49	3.2907
4.5	43.301	143.29	3.3091
5.0	43.301	141.47	3.2671



**Figure 4.14:** Stress Concentration Factor,  $K$  vs  $L/d_n$  for  $r_n/t_n = 10$

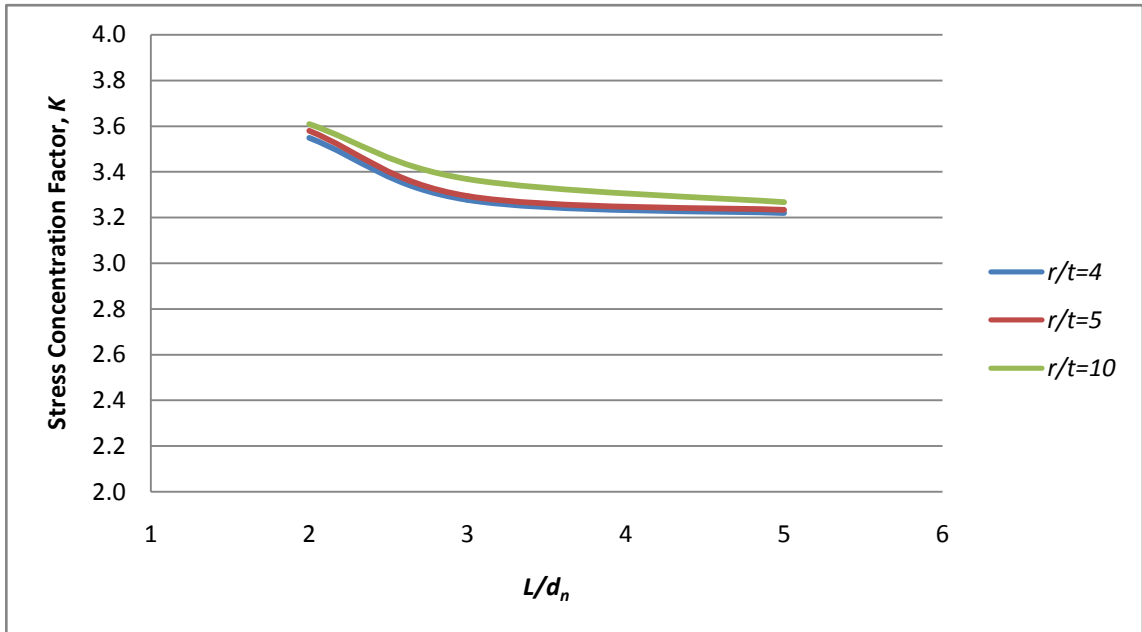
From simulation, the maximum stress occurred at the junction of nozzles-vessel.

Figure 4.15 shows a sample of ANSYS simulation for nozzles 30° from one another.



**Figure 4.15:** Samples of ANSYS simulation for nozzles 30° from one another

Figure 4.16 below shows the overall result for nozzles  $30^\circ$  from one another.



**Figure 4.16:** Stress Concentration Factor,  $K$  vs  $L/d_n$  for nozzles  $30^\circ$  from one another.

The rest of the simulation results for nozzles  $30^\circ$  from one another are attached in the Appendices. In short, the maximum stress occurs at the junction of pressure vessel-nozzles because the state of stress there is significantly greater due to the geometric discontinuities caused by the holes. The value of stress concentration factor,  $K$  will decrease as the result of increasing the center to center distance,  $L$  between the two nozzles. It also decreases with the increase of the thickness of the nozzles,  $t_n$ .

#### 4.5.4 Results for nozzles 45° from one another.

This is the result for the condition where nozzles are 45° from one another.

Table 4.18 and Figure 4.17 shows the result for  $r_n/t_n = 4$ .

**Table 4.18:** Results for nozzles 45° from one another for  $r_n/t_n = 4$

$L/d_n$	Average Stress (MPa)	Maximum Stress ( MPa)	Stress Concentration Factor, K
2.0	43.301	148.17	3.4219
2.5	43.301	146.17	3.3758
3.0	43.301	139.56	3.2230
3.5	43.301	135.90	3.1385
4.0	43.301	141.05	3.2574
4.5	43.301	140.06	3.2345
5.0	43.301	135.47	3.1286

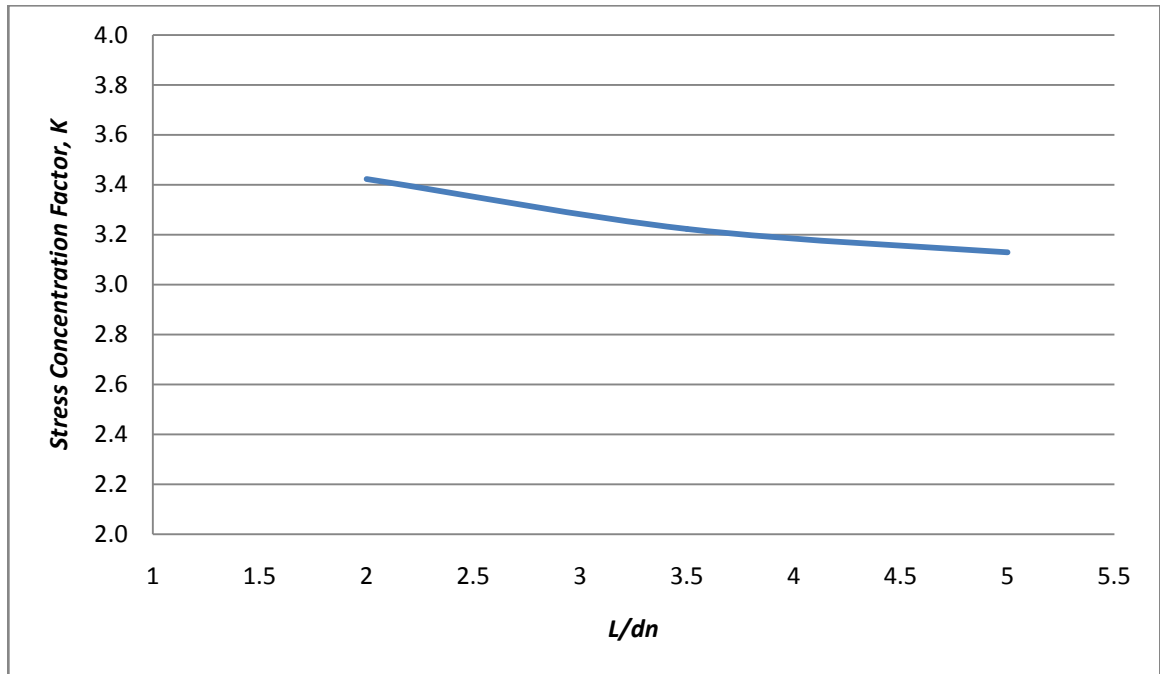


**Figure 4.17:** Stress Concentration Factor, K vs  $L/d_n$  for  $r_n/t_n = 4$

Table 4.19 and Figure 4.18 shows the result for  $r_n/t_n = 5$ .

**Table 4.19:** Results for nozzles  $45^\circ$  from one another for  $r_n/t_n = 5$

$L/d_n$	Average Stress (MPa)	Maximum Stress ( MPa)	Stress Concentration Factor, K
2.0	43.301	153.83	3.5526
2.5	43.301	144.43	3.3355
3.0	43.301	144.48	3.3366
3.5	43.301	136.64	3.1556
4.0	43.301	141.64	3.2711
4.5	43.301	140.55	3.2489
5.0	43.301	140.22	3.2383

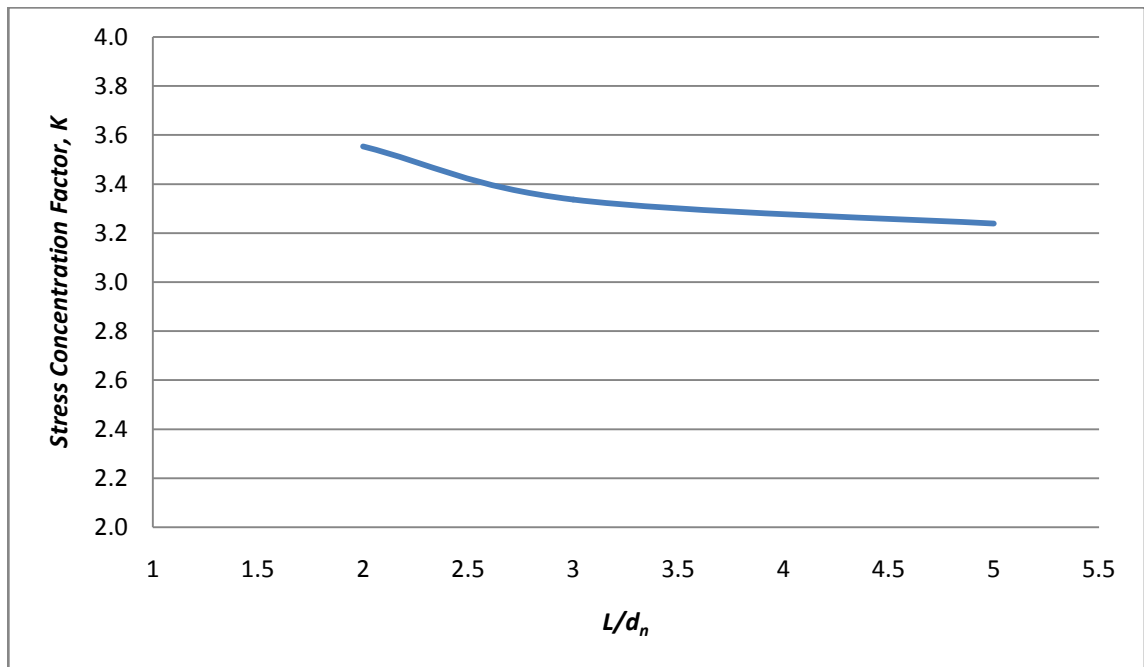
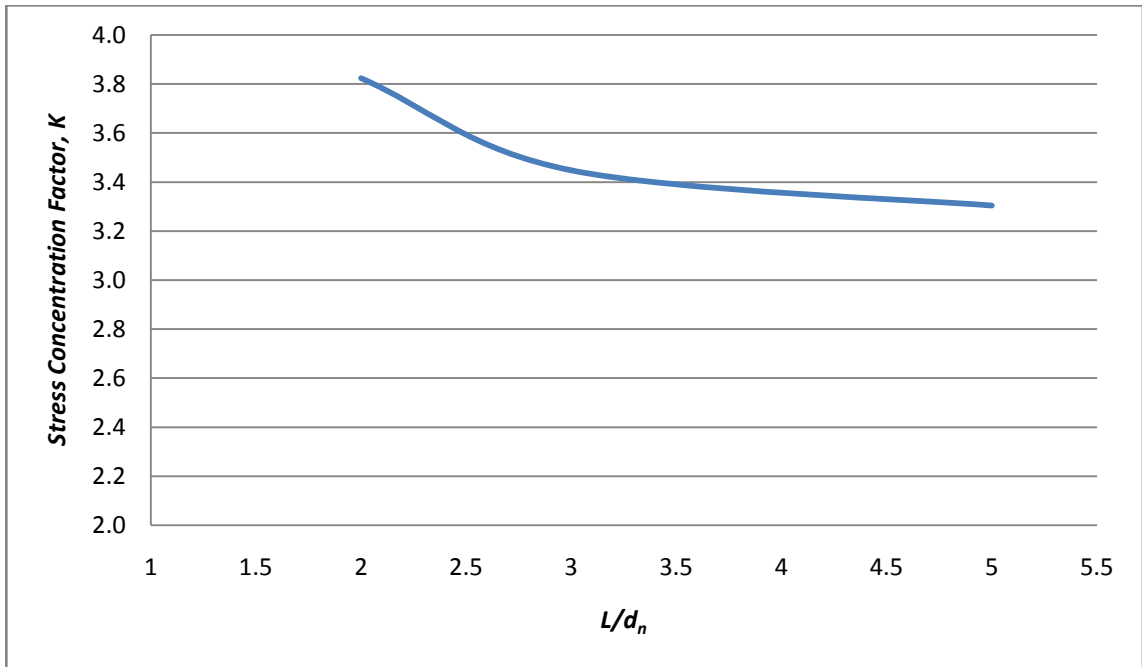


**Figure 4.18:** Stress Concentration Factor,  $K$  vs  $L/d_n$  for  $r_n/t_n = 5$

Table 4.20 and Figure 4.19 shows the result for  $r_n/t_n = 10$ .

**Table 4.20:** Results for nozzles  $45^\circ$  from one another for  $r_n/t_n = 10$

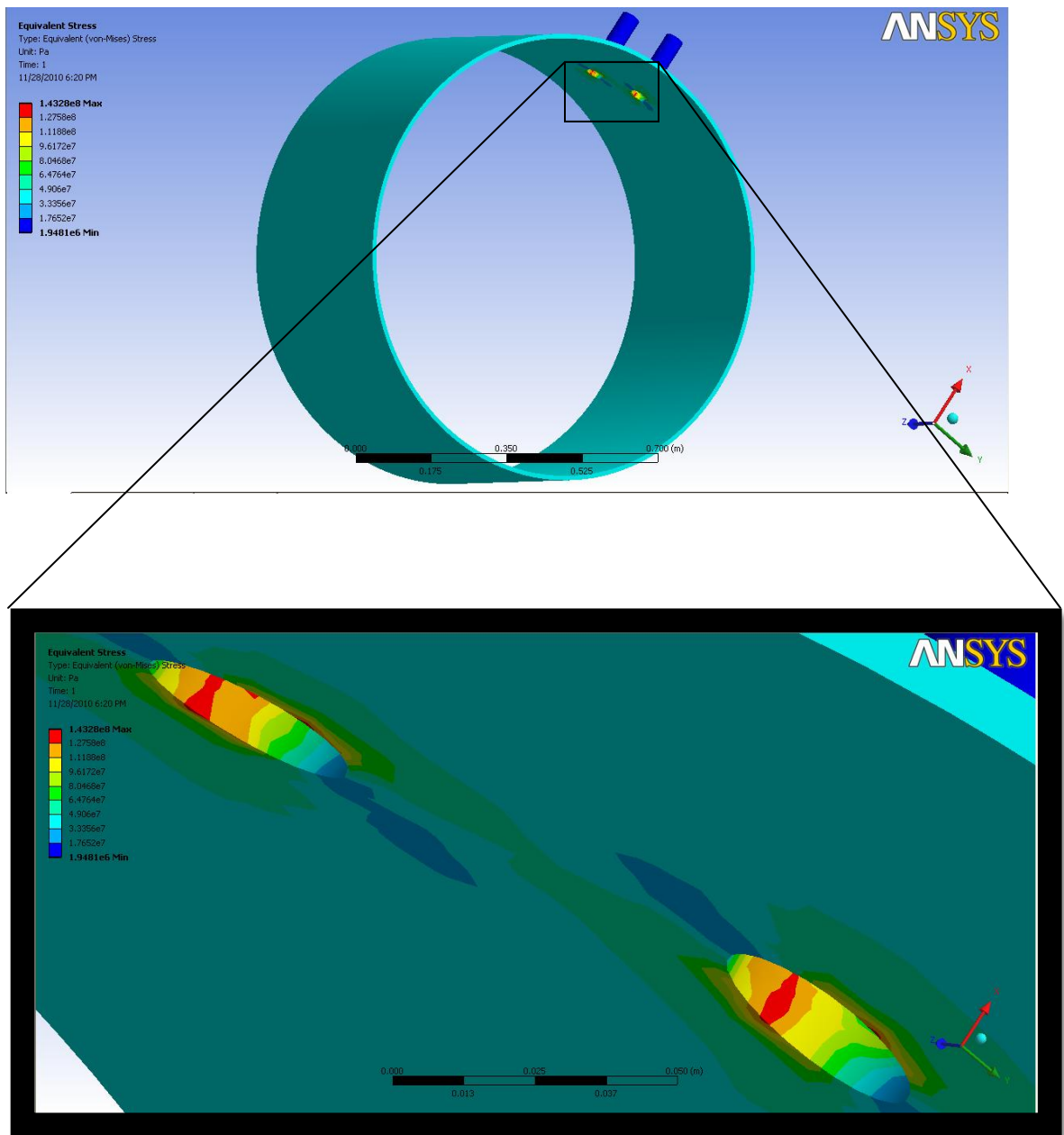
$L/d_n$	Average Stress (MPa)	Maximum Stress ( MPa)	Stress Concentration Factor, K
2.0	43.301	165.55	3.8232
2.5	43.301	157.93	3.6473
3.0	43.301	149.28	3.4475
3.5	43.301	144.96	3.3477
4.0	43.301	146.38	3.3805
4.5	43.301	147.90	3.4156
5.0	43.301	143.03	3.3032



**Figure 4.19:** Stress Concentration Factor,  $K$  vs  $L/d_n$  for  $r_n/t_n = 10$

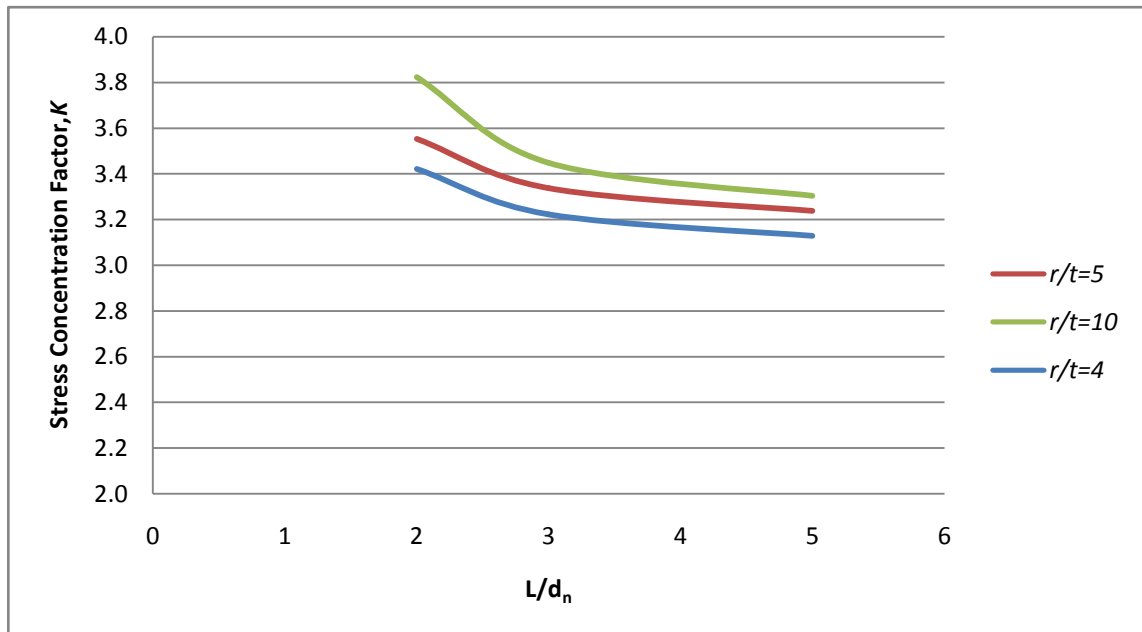
From simulation, the maximum stress occurred at the junction of nozzles-vessel.

Figure 4.20 shows a sample of ANSYS simulation for nozzles 45° from one another.



**Figure 4.20:** Samples of ANSYS simulation for nozzles 45° from one another

Figure 4.21 below shows the overall result for nozzles  $45^\circ$  from one another.



**Figure 4.21:** Stress Concentration Factor,  $K$  vs  $L/d_n$  for nozzles  $45^\circ$  from one another

The rest of the simulation results for nozzles  $45^\circ$  from one another are attached in the Appendices. In short, the maximum stress occurs at the junction of pressure vessel-nozzles because the state of stress there is significantly greater due to the geometric discontinuities caused by the holes. The value of stress concentration factor,  $K$  will decrease as the result of increasing the center to center distance,  $L$  between the two nozzles. It also decreases with the increase of the thickness of the nozzles,  $t_n$ .

#### 4.5.4 Results for nozzles 60° from one another

This is the result for the condition where nozzles are 60° from one another.

Table 4.21 and Figure 4.22 shows the result for  $r_n/t_n = 4$ .

**Table 4.21:** Results for nozzles 60° from one another for  $r_n/t_n = 4$

$L/d_n$	Average Stress (MPa)	Maximum Stress ( MPa)	Stress Concentration Factor, K
2.0	43.301	144.71	3.3420
2.5	43.301	138.63	3.1600
3.0	43.301	140.04	3.2341
3.5	43.301	139.21	3.2149
4.0	43.301	138.11	3.1895
4.5	43.301	140.76	3.2507
5.0	43.301	138.84	3.2063

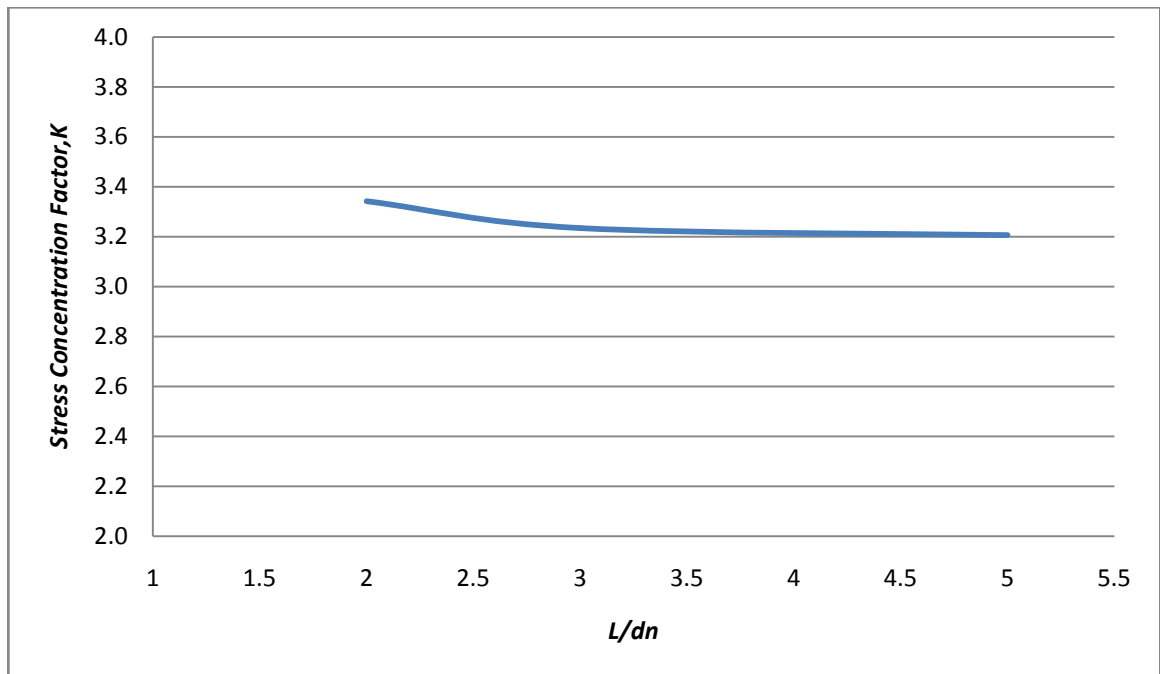


**Figure 4.22:** Stress Concentration Factor, K vs  $L/d_n$  for  $r_n/t_n = 4$

Table 4.22 and Figure 4.23 shows the result for  $r_n/t_n = 5$ .

**Table 4.22:** Results for nozzles  $60^\circ$  from one another for  $r_n/t_n = 5$

$L/d_n$	Average Stress (MPa)	Maximum Stress ( MPa)	Stress Concentration Factor, K
2.0	43.301	146.16	3.3754
2.5	43.301	138.17	3.1909
3.0	43.301	140.04	3.2341
3.5	43.301	139.88	3.2304
4.0	43.301	137.69	3.1798
4.5	43.301	141.62	3.2706
5.0	43.301	140.40	3.2424

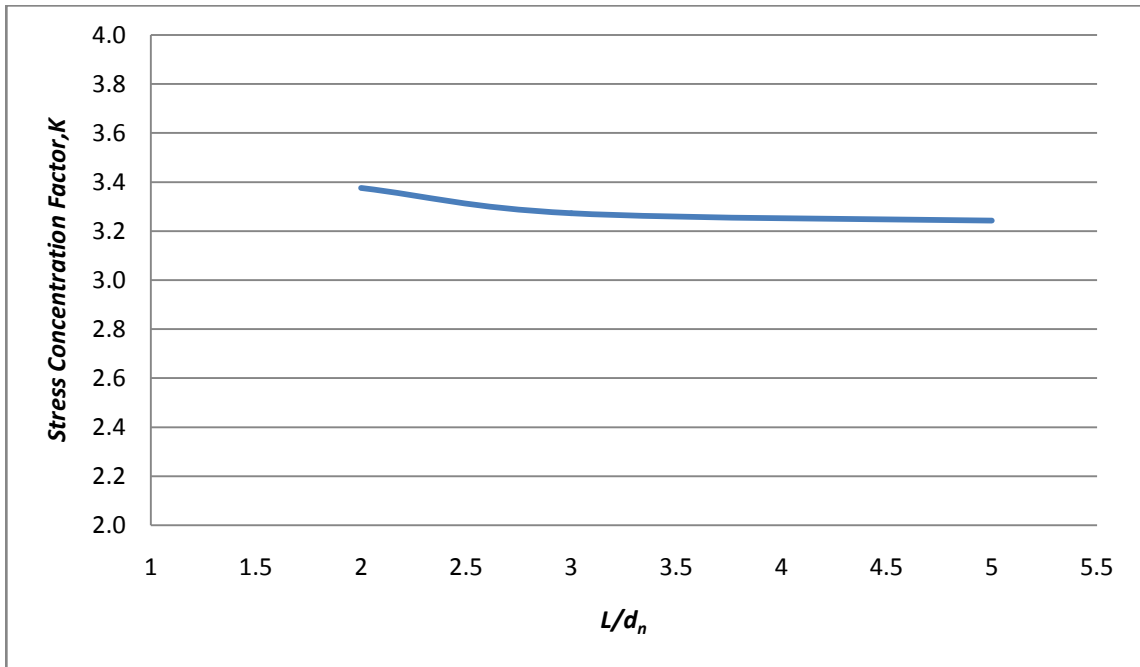
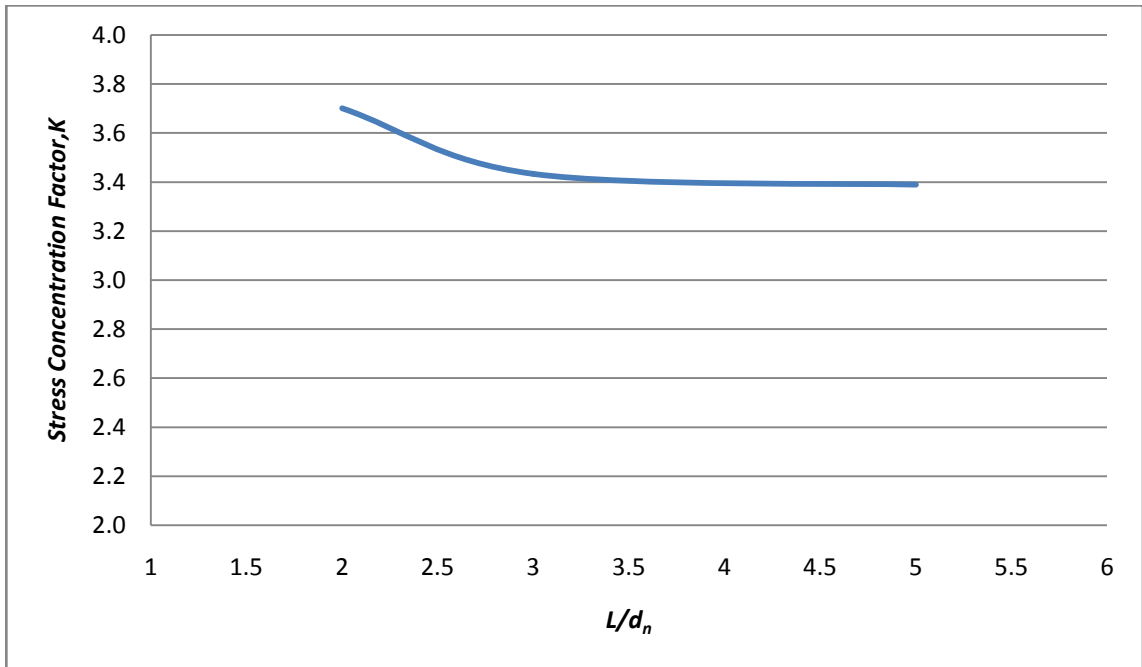


**Figure 4.23:** Stress Concentration Factor,  $K$  vs  $L/d_n$  for  $r_n/t_n = 5$

Table 4.23 and Figure 4.24 shows the result for  $r_n/t_n = 10$ .

**Table 4.23:** Results for nozzles  $60^\circ$  from one another for  $r_n/t_n = 10$

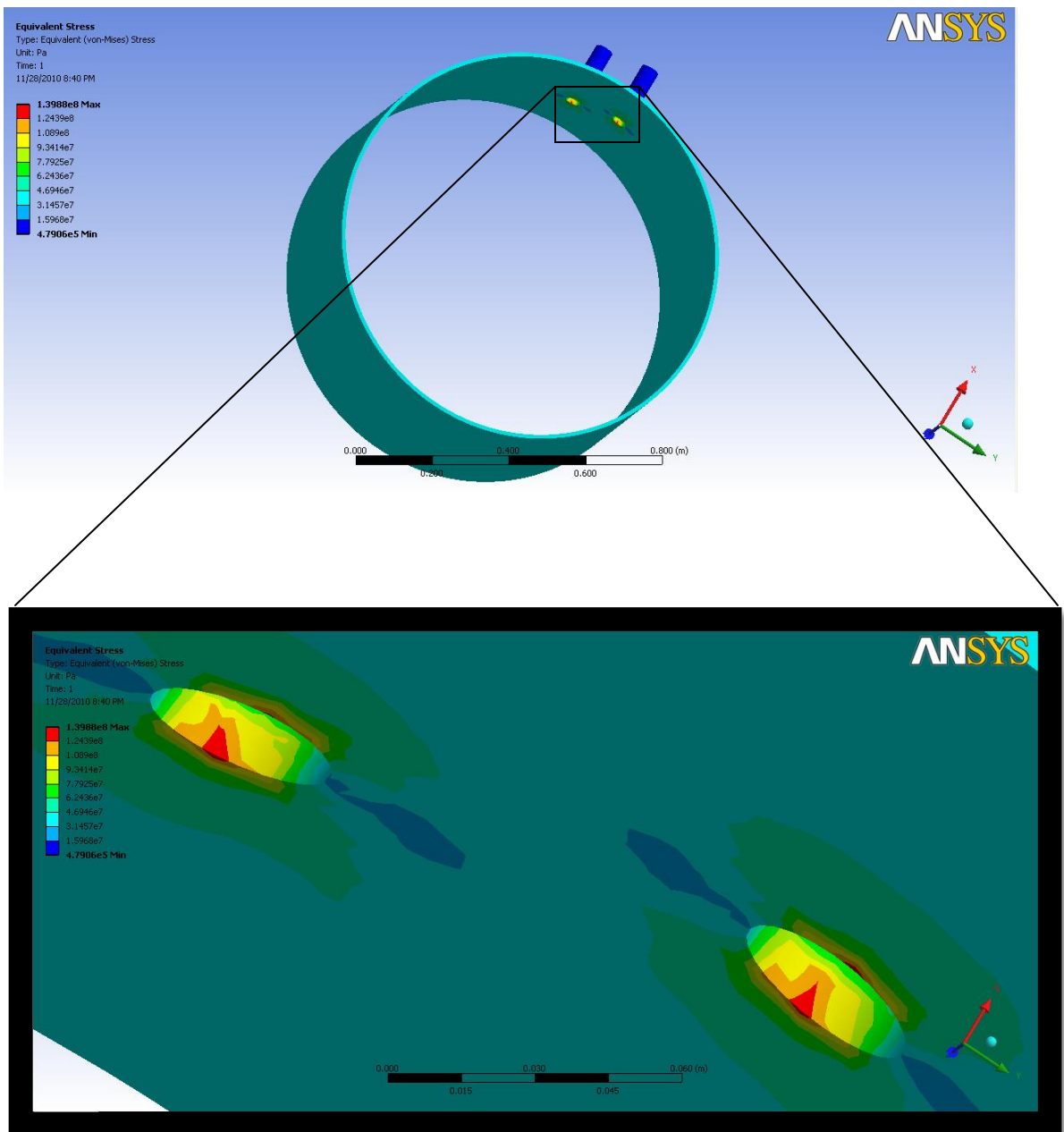
$L/d_n$	Average Stress (MPa)	Maximum Stress ( MPa)	Stress Concentration Factor, K
2.0	43.301	160.23	3.7004
2.5	43.301	148.64	3.4327
3.0	43.301	148.65	3.4329
3.5	43.301	153.22	3.5385
4.0	43.301	145.04	3.3496
4.5	43.301	145.97	3.3711
5.0	43.301	146.76	3.3892



**Figure 4.24:** Stress Concentration Factor,  $K$  vs  $L/d_n$  for  $r_n/t_n = 10$

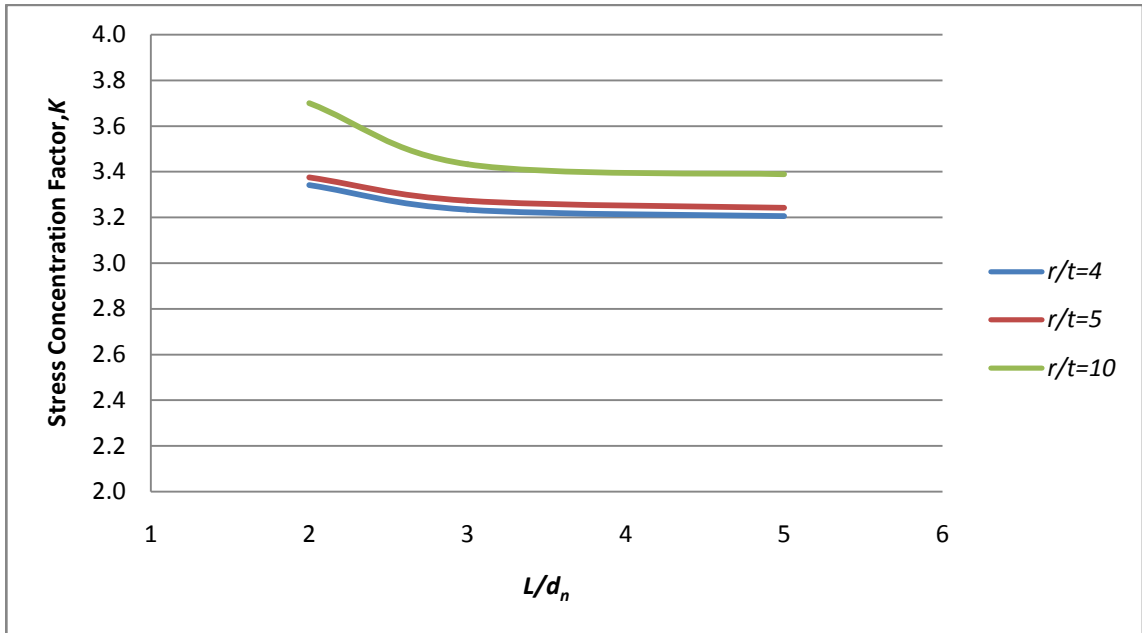
From simulation, the maximum stress occurred at the junction of nozzles-vessel.

Figure 4.25 shows a sample of ANSYS simulation for nozzles  $60^\circ$  from one another.



**Figure 4.25:** Samples of ANSYS simulation for nozzles  $60^\circ$  from one another

Figure 4.26 below shows the overall result for nozzles  $60^\circ$  from one another.



**Figure 4.26:** Stress Concentration Factor,  $K$  vs  $L/d_n$  for nozzles  $60^\circ$  from one another

The rest of the simulation results for nozzles  $60^\circ$  from one another are attached in the Appendices. In short, the maximum stress occurs at the junction of pressure vessel-nozzles because the state of stress there is significantly greater due to the geometric discontinuities caused by the holes. The value of stress concentration factor,  $K$  will decrease as the result of increasing the center to center distance,  $L$  between the two nozzles. It also decreases with the increase of the thickness of the nozzles,  $t_n$ .

## CHAPTER 5

### CONCLUSIONS

Specific values of stress concentration factor,  $K$ , are generally reported in graphical form in handbooks related to stress analysis. However, the information regarding stress concentration factor are limited to 1-dimensional and 2-dimensional problems. On the other hand, most real world parts and assemblies are far too complex to do accurately without the use of a computer and appropriate analysis software. Thus, this project provides the data necessary for stress concentration factor at two adjacent nozzles in a cylindrical pressure vessel that is very useful to designers.

The initial stage of this project in doing research and study on previous literature had given a better understanding on the stress concentration in a cylindrical pressure vessel. However, there are some difficulties in finding the appropriate journals or previous work related to the design of cylindrical pressure vessel. The stress distribution of a cylindrical pressure vessel with two adjacent nozzles are investigated by using finite element method by varying center to center distance of the nozzles,  $L$ , over the diameter of the nozzles,  $d_n$  ratios for different nozzles thickness,  $t_n$ , to nozzles radius,  $r_n$  ratios.

In short, the maximum stress occurs at the junction of pressure vessel-nozzles because at this junction, the state of stress there is significantly greater due to the geometric discontinuities cause by the holes. The project has achieved the objective which is to investigate and to plot the diagram for the stress distribution at two adjacent nozzles in a cylindrical pressure vessel.

## REFERENCES

1. Stress Concentration by David Grieve. 8 April 2008. Taken September, 24 2010 .Website : <http://www.tech.plym.ac.uk/sme/desnotes/stressconc.htm>
2. Stress Concentration Factor. Taken September,24 2010 .Website : [http://en.wikipedia.org/wiki/Stress\\_concentration\\_factor](http://en.wikipedia.org/wiki/Stress_concentration_factor)
3. Joseph Edward Shigley, Charles R. Mischke and Richard G. Budynas 2003, *Mechanical Engineering Design*, 7th edition, McGraw-Hill Science Engineering
4. Mechanical Engineering Design; Stress Concentration. Taken September, 24 2010.  
Website:[http://highered.mcgraw-hill.com/sites/dl/free/0072520361/82833/Ch04\\_Section14\\_Stress\\_Concentration.pdf](http://highered.mcgraw-hill.com/sites/dl/free/0072520361/82833/Ch04_Section14_Stress_Concentration.pdf)
5. Hibbeler R.C. 2005, *Mechanics of Materials*, Singapore, Prentice Hall
6. Thin Walled Pressure Vessel. Taken September, 24 2010.Website : <http://courses.washington.edu/me354a/Thin%20Walled%20Pressure%20vessels.pdf>
7. Ku Nawwar binti Ku Khalid, “ Stress Concentration Factor at Two Longitudinal Adjacent Nozzles in a Cylindrical Pressure Vessel”, Interim Report, Bachelor of Mechanical Engineering, Universiti Teknologi PETRONAS, December 2009
8. Stress Concentration Analysis and Design. Taken September,24 2010.Website : [http://www.knovel.com/web/portal/browse/display?\\_EXT\\_KNOVEL\\_DISPLAY\\_bookid=583](http://www.knovel.com/web/portal/browse/display?_EXT_KNOVEL_DISPLAY_bookid=583)
9. W.D. Growney 2008, “2008 International ANSYS Conference”, “*Using FEA Results To Determine Stress Concentration Factors*”, W.D. Growney ,Engineering Specialist, Eaton Aerospace, Conveyance Systems Division
10. Estimation of Stress Concentrations.Taken September,24 2010.Website : <http://www.fesb.hr/~djelaska/documents/FSCF98.pdf>
11. Stress Concentration Factors. Taken September, 24 2010 .Website: <http://www.mae.ufl.edu/haftka/structures/stressconc.pdf>.

12. **Moaveni S.** 2003, *Finite Element Analysis: Theory and Application with ANSYS*, New Jersey, Pearson Education.
13. John Spence, A. S. Tooth;1994, *Pressure Vessel Design:Concept and Principles*, Taylor & Francis, 1994 - Technology & Engineering
14. Walter D. Pilkey, Deborah F. Pilkey, Rudolph Earl Peterson; 2008, *Stress Concentration Factor*,John Wiley and Son.
15. DEKKER C. J. <sup>(1)</sup>; STIKVOORT W. J. <sup>(2)</sup>; 1997, International journal of pressure vessels and piping, Elsevier, Oxford, ROYAUME-UN.
16. Stress Concentration Factor.Taken September, 24 2010. Website:  
[http://www.mae.ncsu.edu/courses/mae316/eischen/docs/Appendix\\_C.pdf](http://www.mae.ncsu.edu/courses/mae316/eischen/docs/Appendix_C.pdf).  
September 24,2010

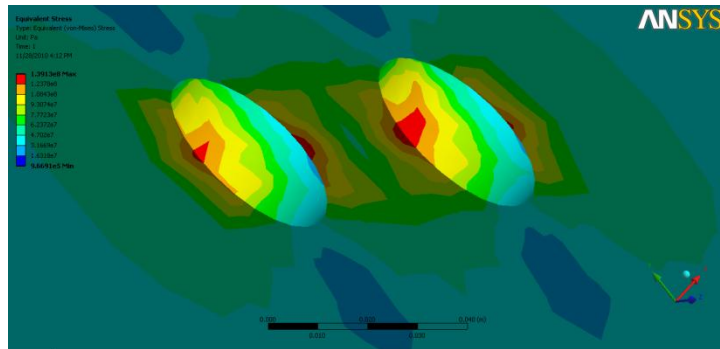
# APPENDICES

## APPENDICES: SIMULATION RESULTS

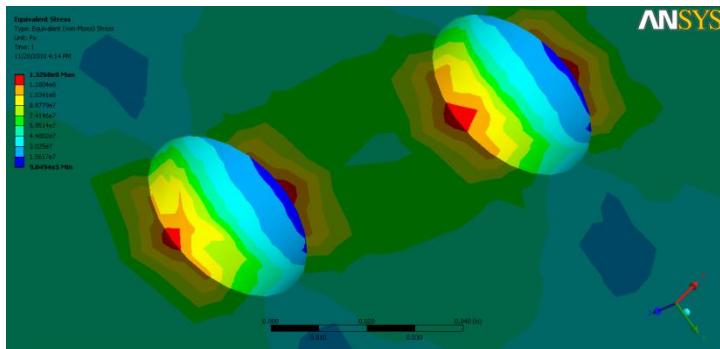
Example of simulation result for nozzles in longitudinal direction

**For  $r_n/t_n = 4$ ;**

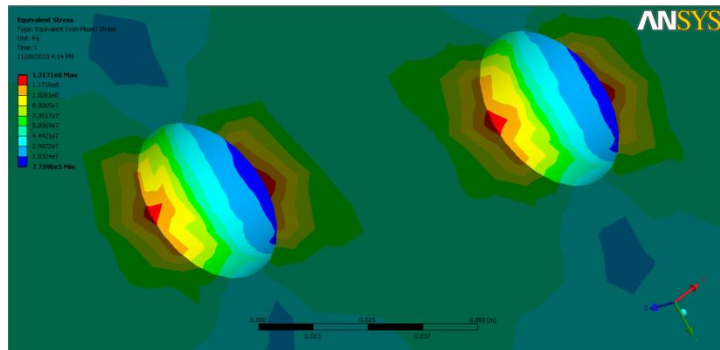
$L/d_n = 2.0$



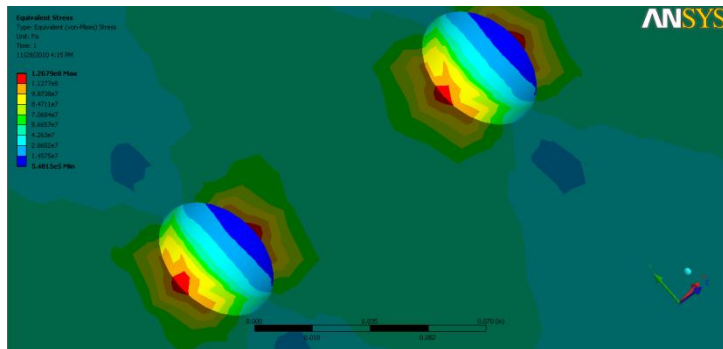
$L/d_n = 2.5$



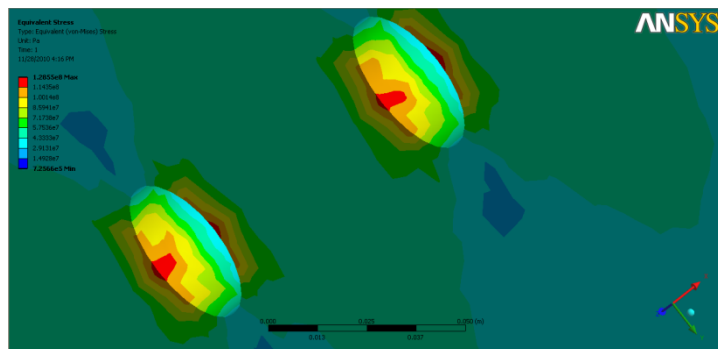
$L/d_n = 3.0$



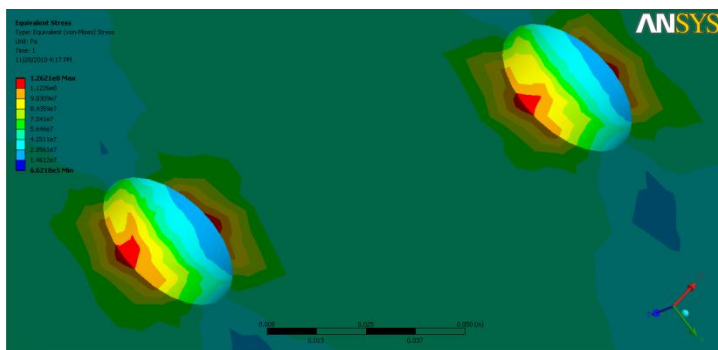
$$L/d_n = 3.5$$



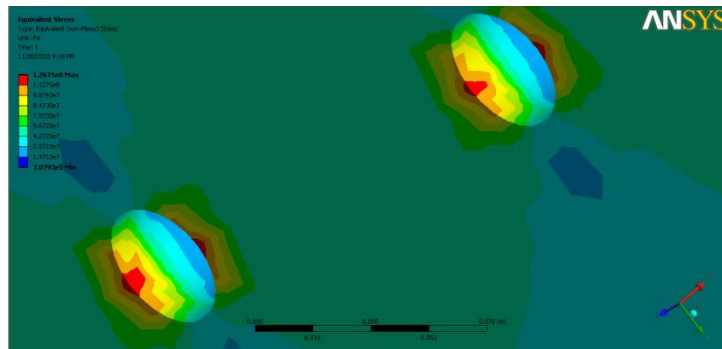
$$L/d_n = 4.0$$



$$L/d_n = 4.5$$

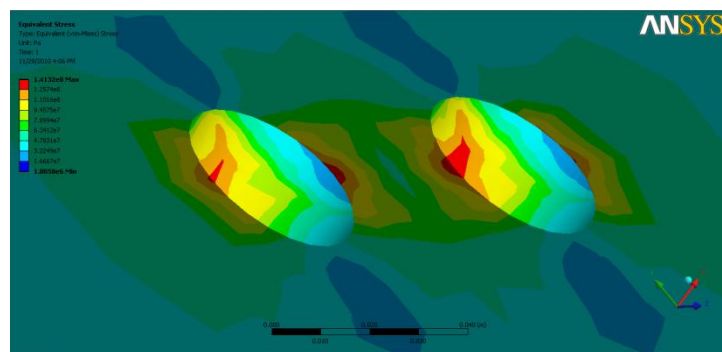


$$L/d_n = 5.0$$

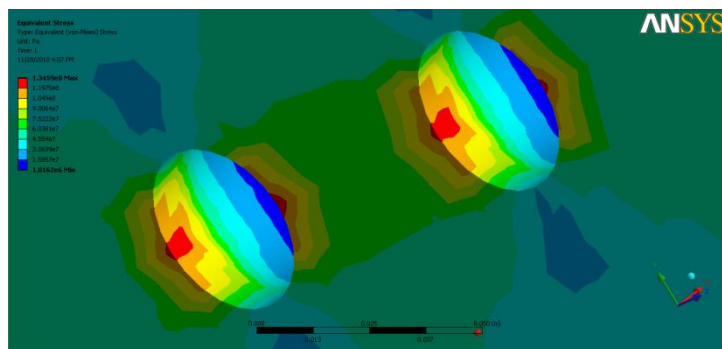


For  $r_n/t_n = 5$ ;

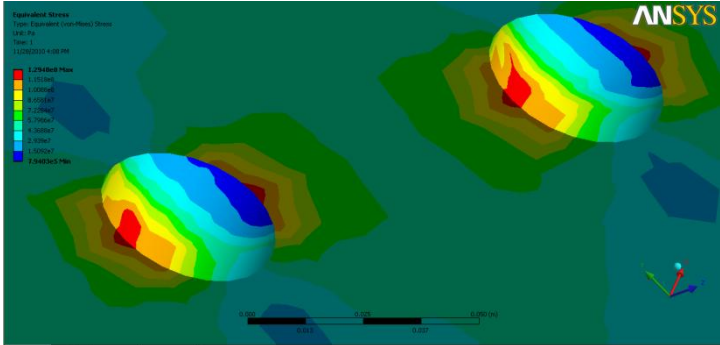
$$L/d_n = 2.0$$



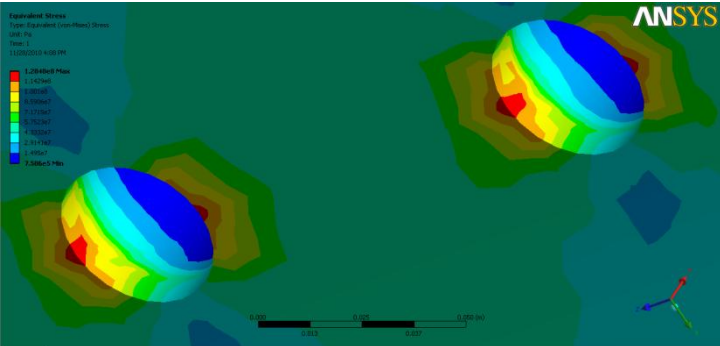
$$L/d_n = 2.5$$



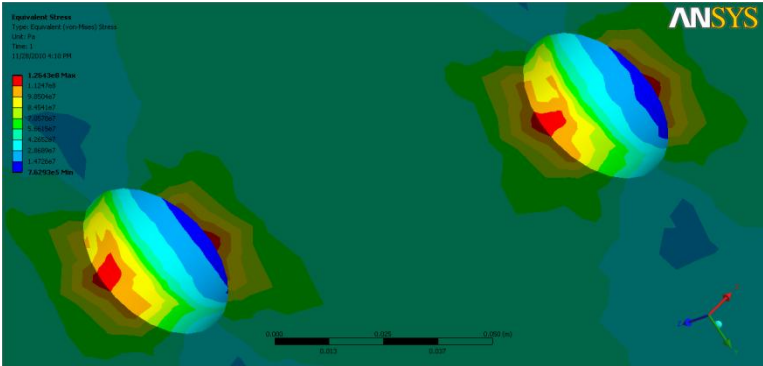
$$L/d_n = 3.0$$



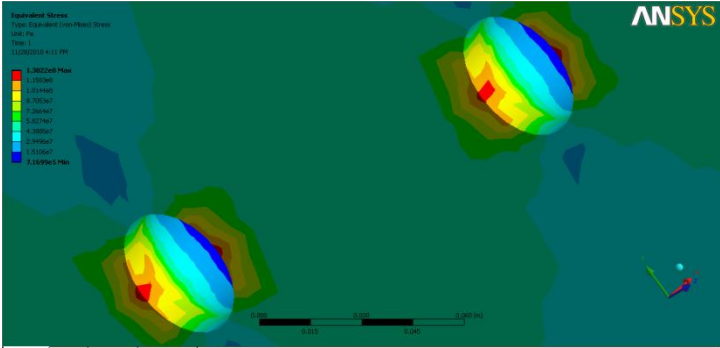
$$L/d_n = 3.5$$



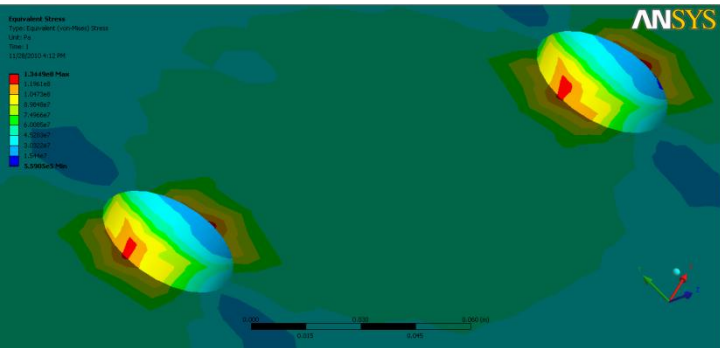
$$L/d_n = 4.0$$



$$L/d_n = 4.5$$

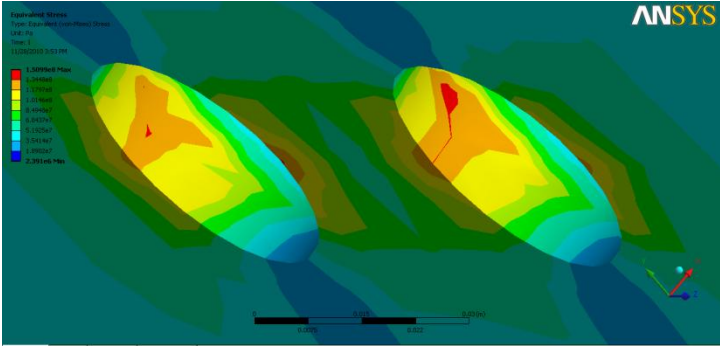


$$L/d_n = 5.0$$

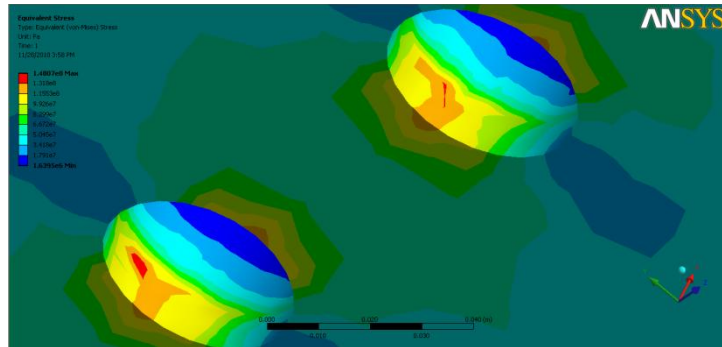


**For  $r_n/t_n = 10$**

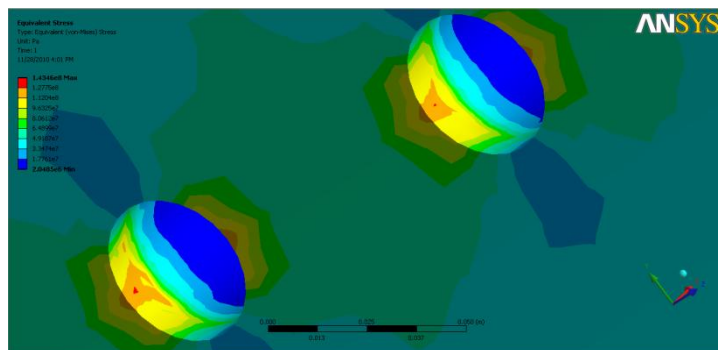
$$L/d_n = 2.0$$



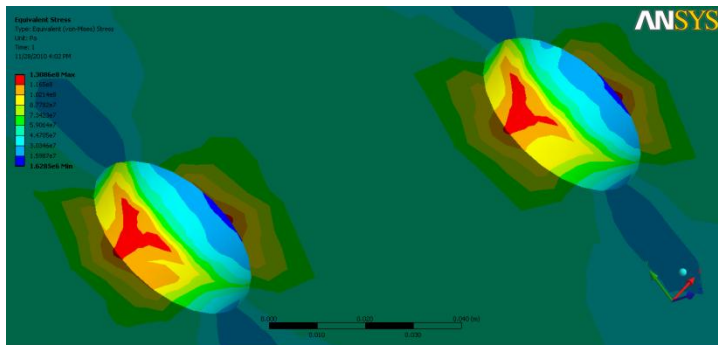
$$L/d_n = 2.5$$



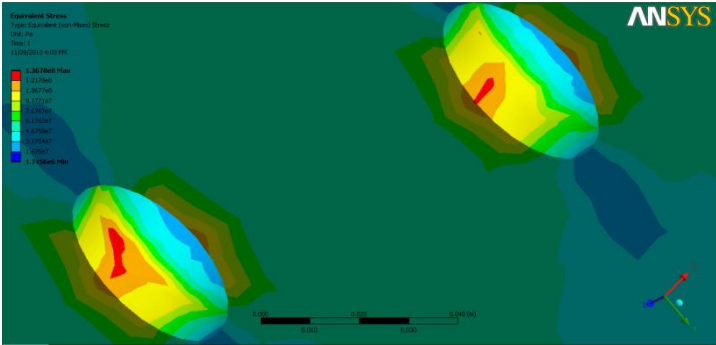
$$L/d_n = 3.0$$



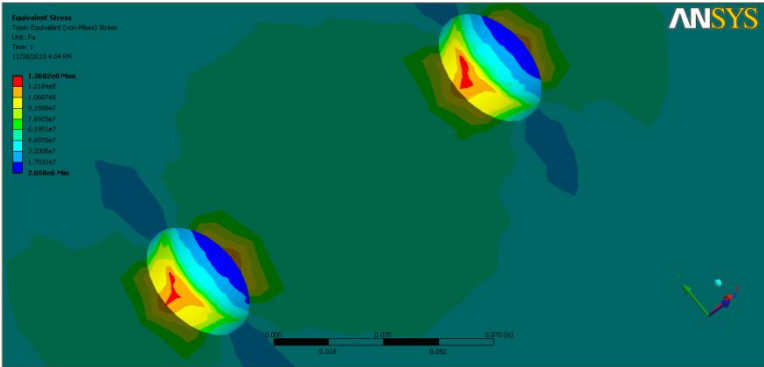
$$L/d_n = 3.5$$



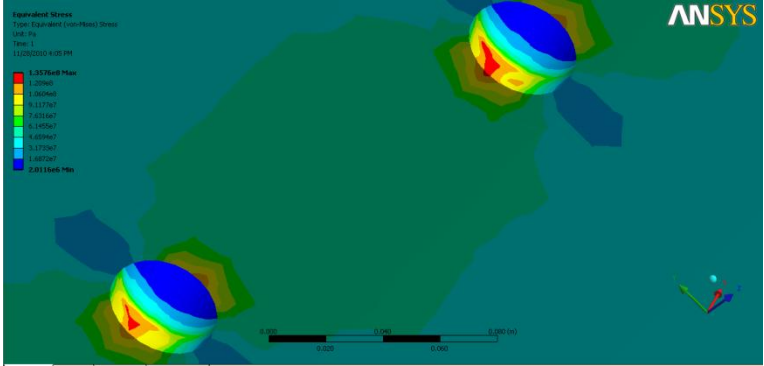
$$L/d_n = 4.0$$



$$L/d_n = 4.5$$



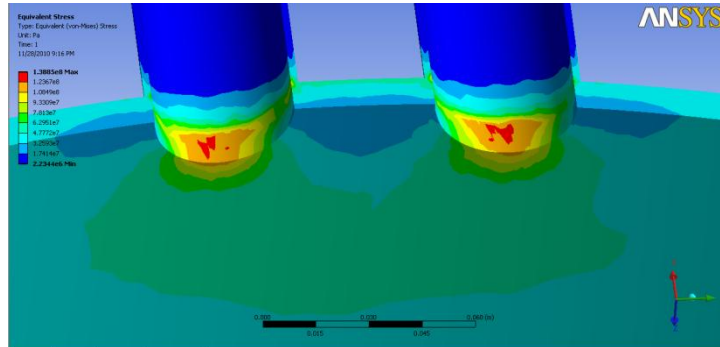
$$L/d_n = 5.0$$



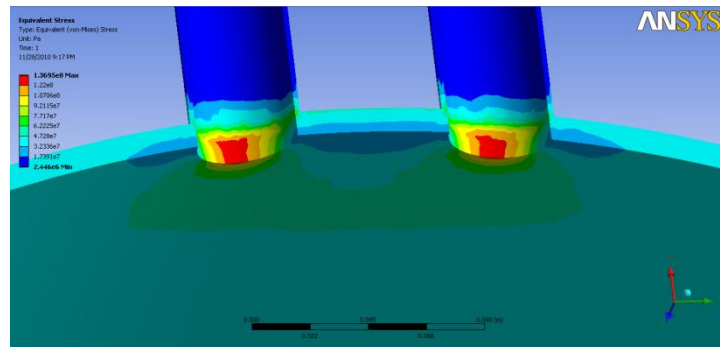
Example of simulation result for nozzles in circumferential direction

**For  $r_n/t_n = 4$ ;**

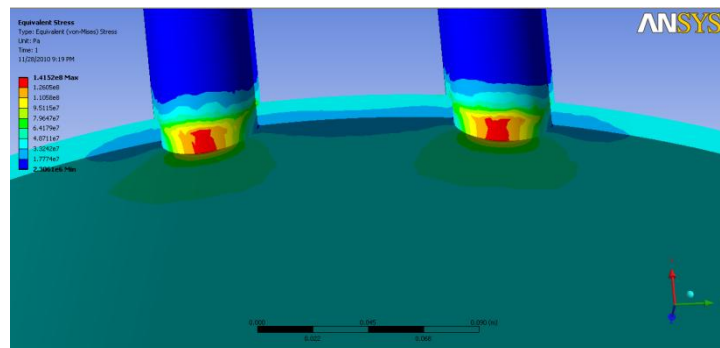
$L/d_n = 2.0$



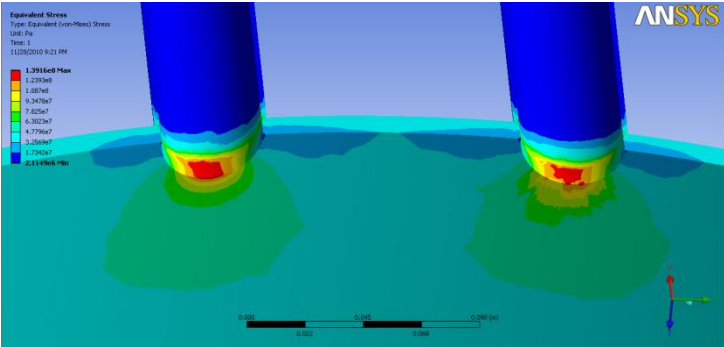
$L/d_n = 2.5$



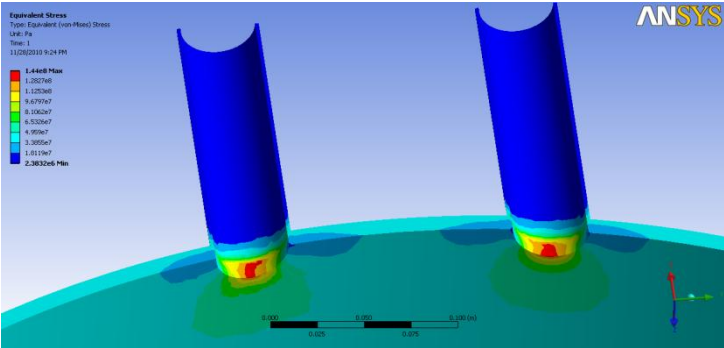
$L/d_n = 3.0$



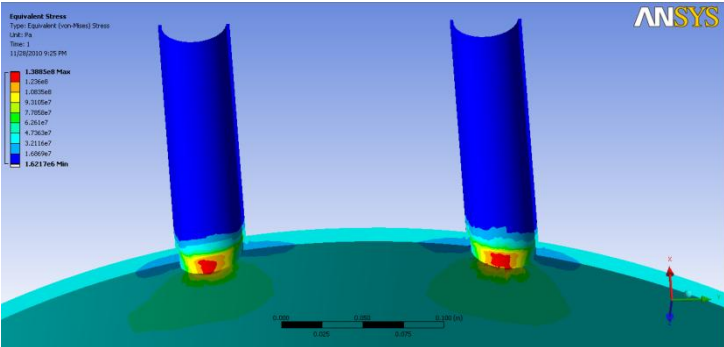
$$L/d_n = 3.5$$



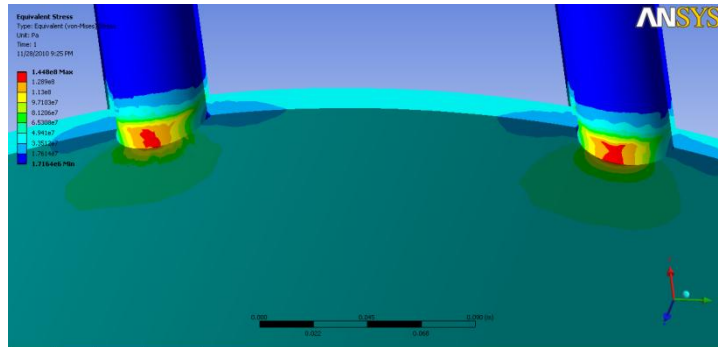
$$L/d_n = 4.0$$



$$L/d_n = 4.5$$

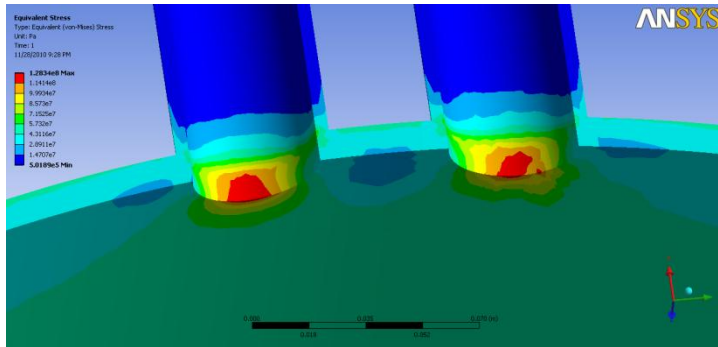


$$L/d_n = 5.0$$

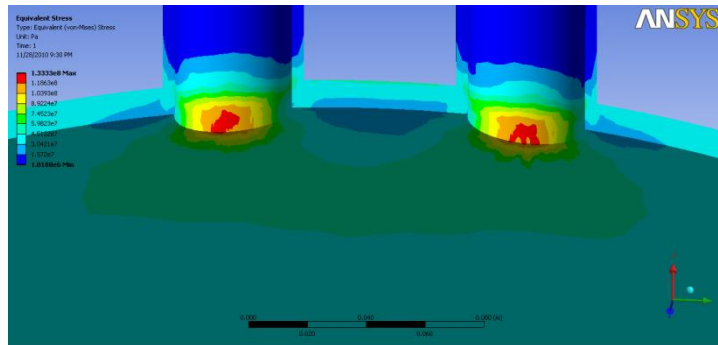


**For  $r_n/t_n = 5$ :**

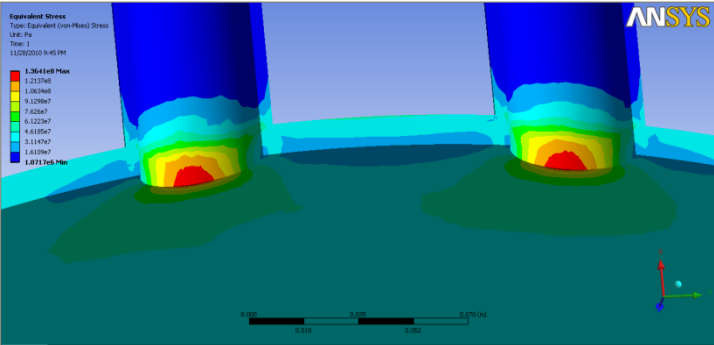
$$L/d_n = 2.0$$



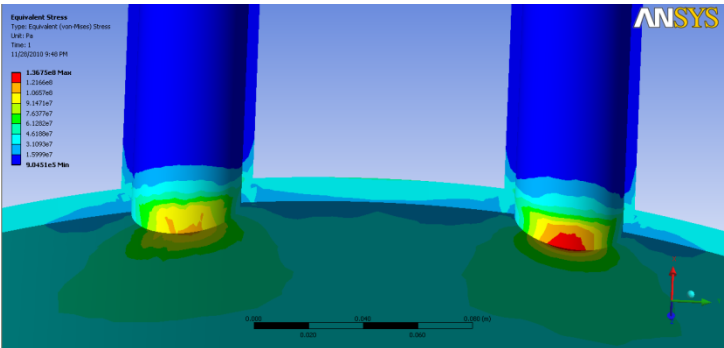
$$L/d_n = 2.5$$



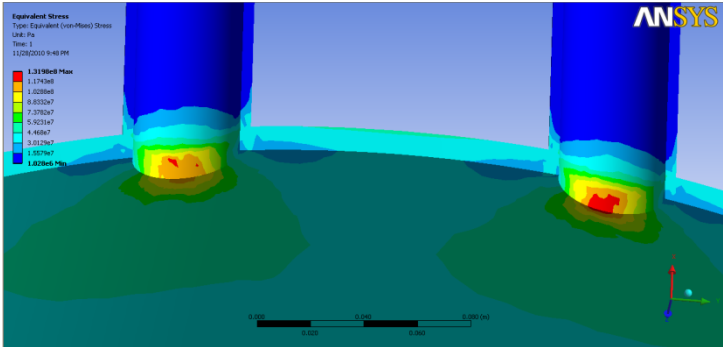
$$L/d_n = 3.0$$



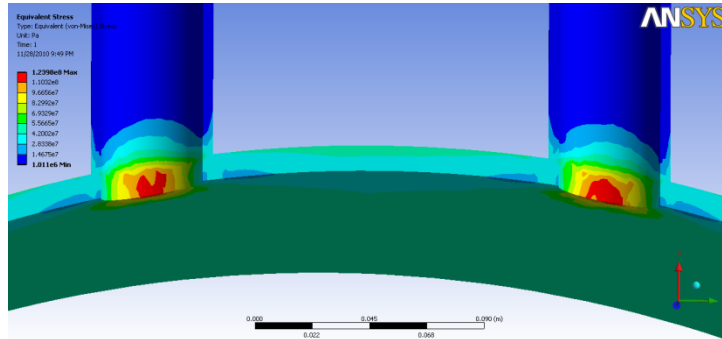
$$L/d_n = 3.5$$



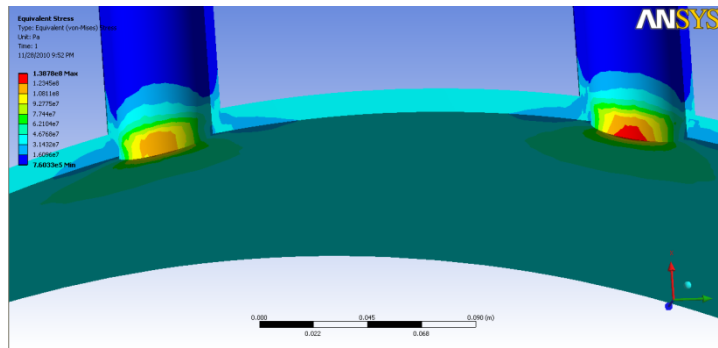
$$L/d_n = 4.0$$



$$L/d_n = 4.5$$

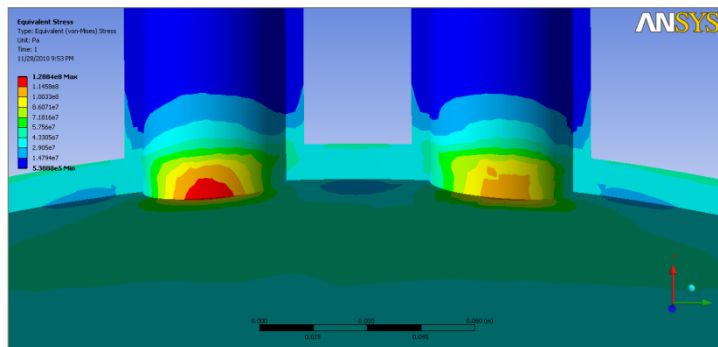


$$L/d_n = 5.0$$

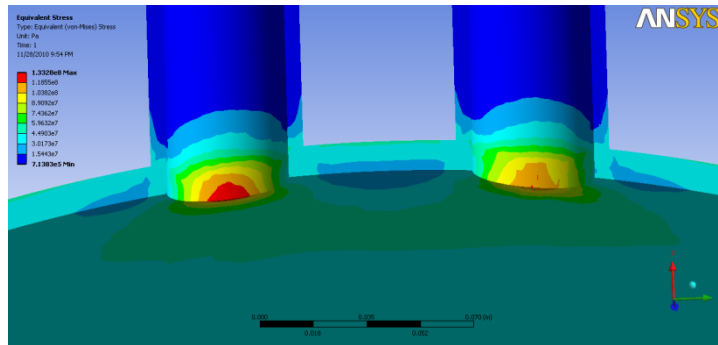


**For  $r_n/t_n = 10$ ;**

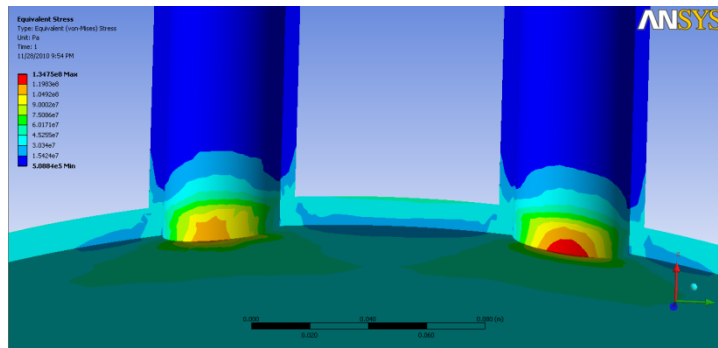
$$L/d_n = 2.0$$



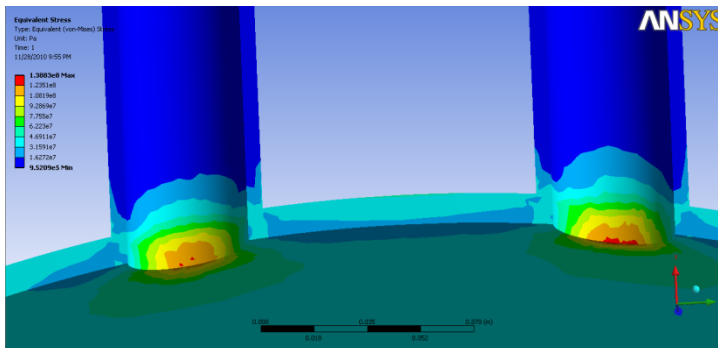
$$L/d_n = 2.5$$



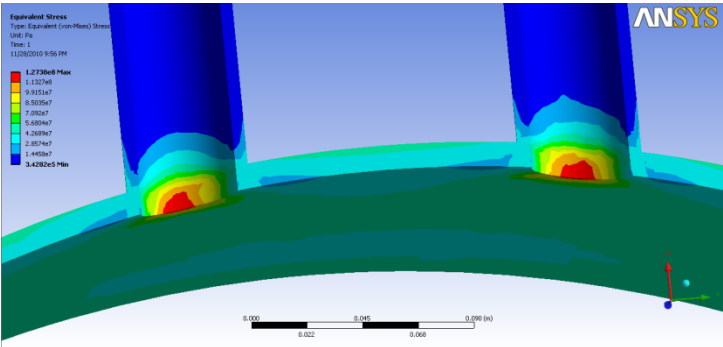
$$L/d_n = 3.0$$



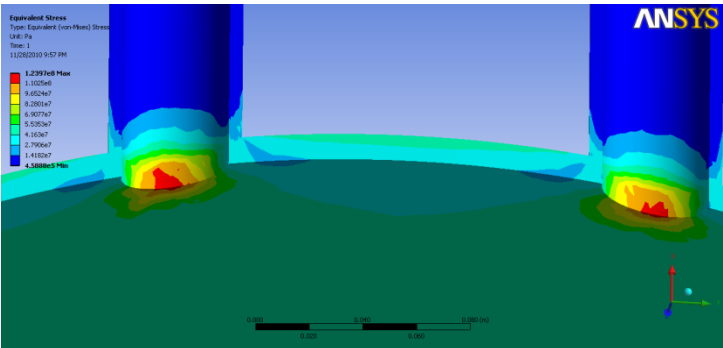
$$L/d_n = 3.5$$



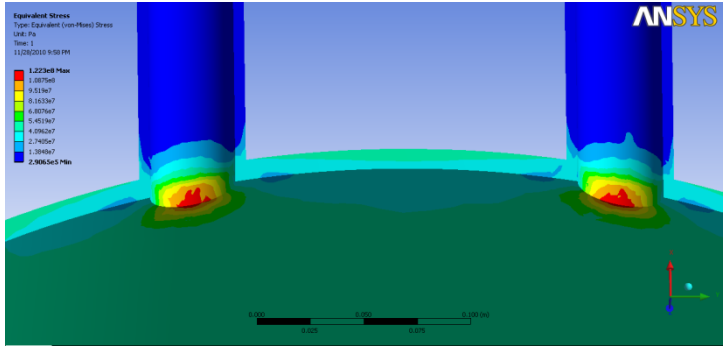
$$L/d_n = 4.0$$



$$L/d_n = 4.5$$



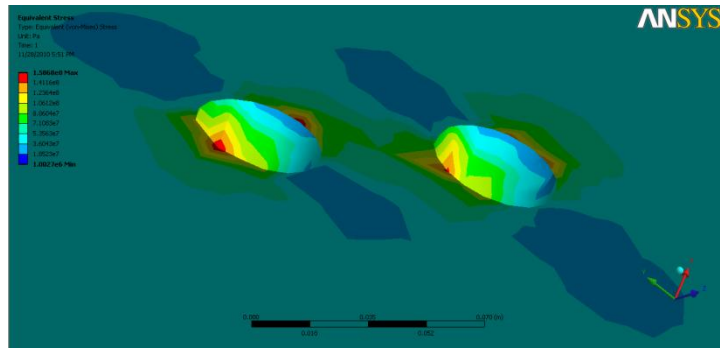
$$L/d_n = 5.0$$



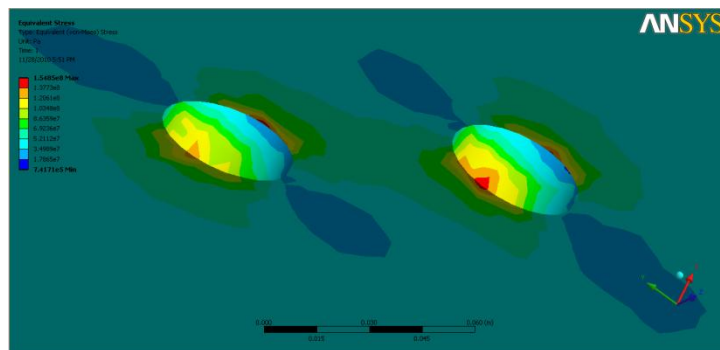
Example of simulation result for nozzles 30° from one another

**For  $r_n/t_n = 4$ ;**

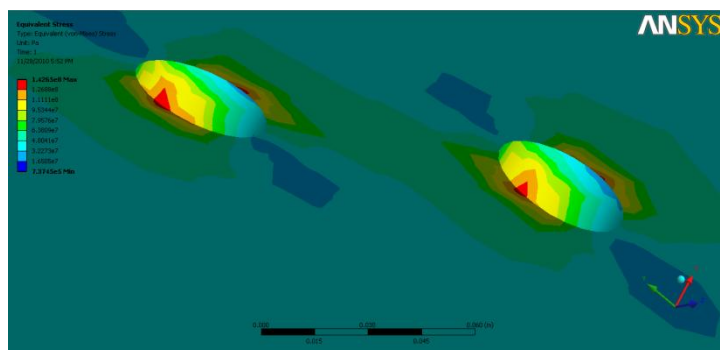
$L/d_n = 2.0$



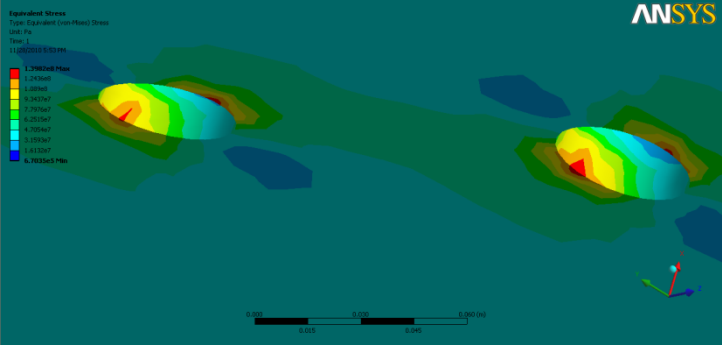
$L/d_n = 2.5$



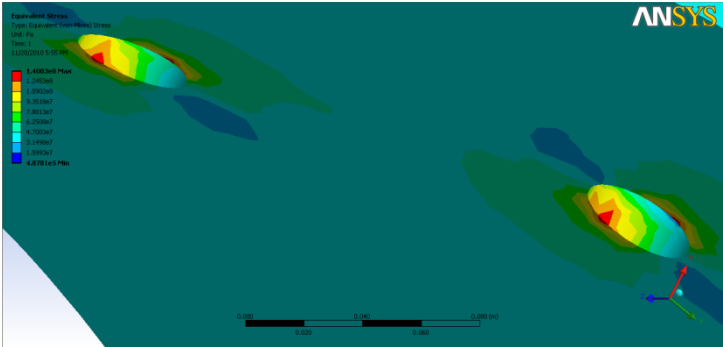
$L/d_n = 3.0$



$$L/d_n = 3.5$$

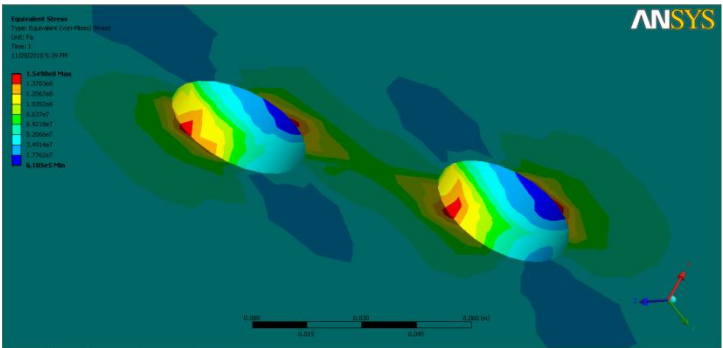


$$L/d_n = 5.0$$

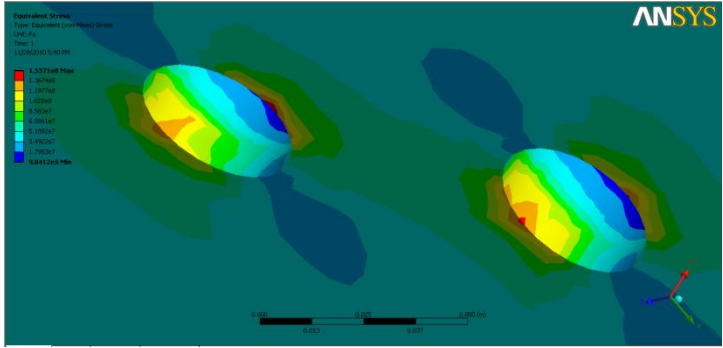


For  $r_n/t_n = 5$ ;

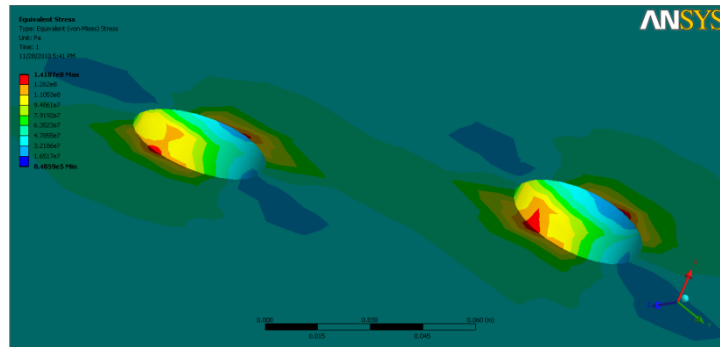
$$L/d_n = 2.0$$



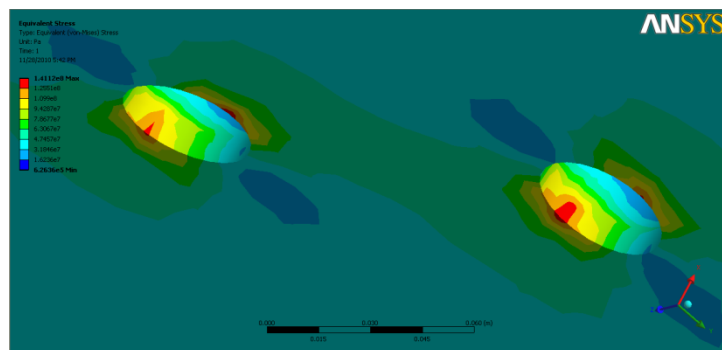
$$L/d_n = 2.5$$



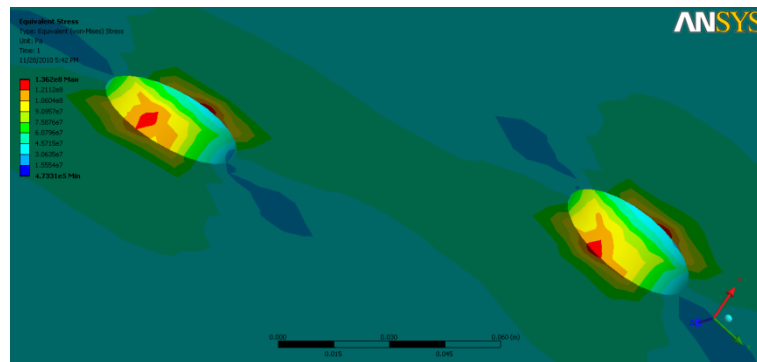
$$L/d_n = 3.0$$



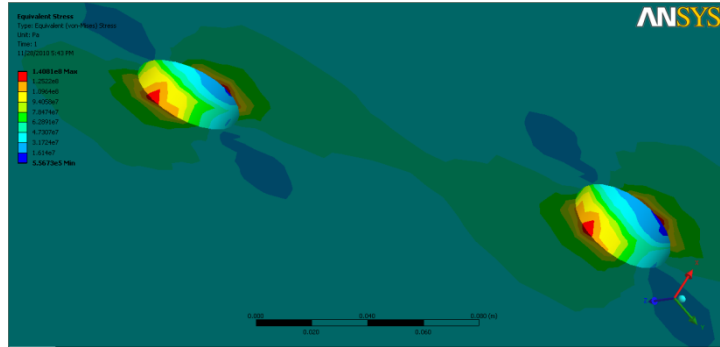
$$L/d_n = 3.5$$



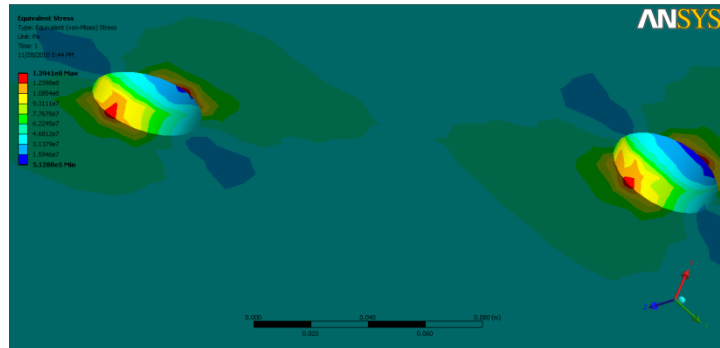
$$L/d_n = 4.0$$



$$L/d_n = 4.5$$

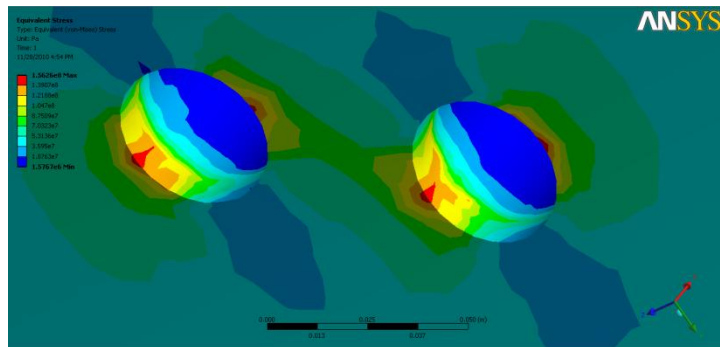


$$L/d_n = 5.0$$

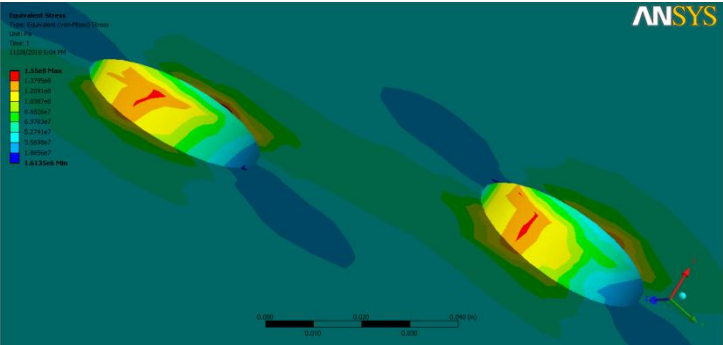


**For  $r_n/t_n = 10$**

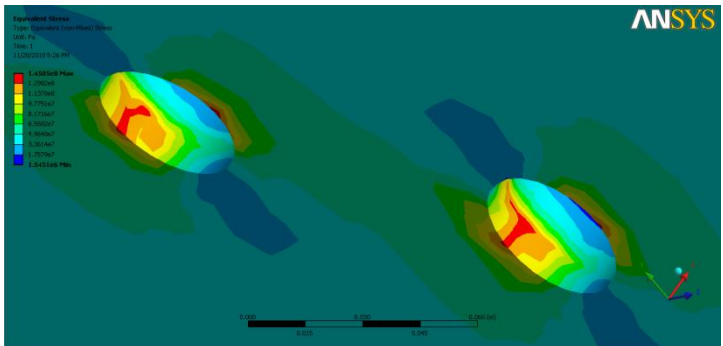
$$L/d_n = 2.0$$



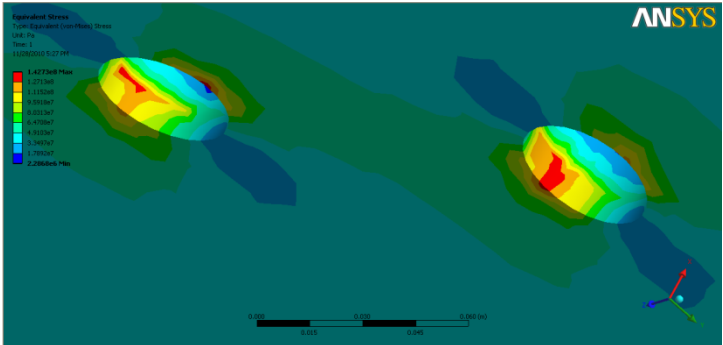
$L/d_n = 2.5$



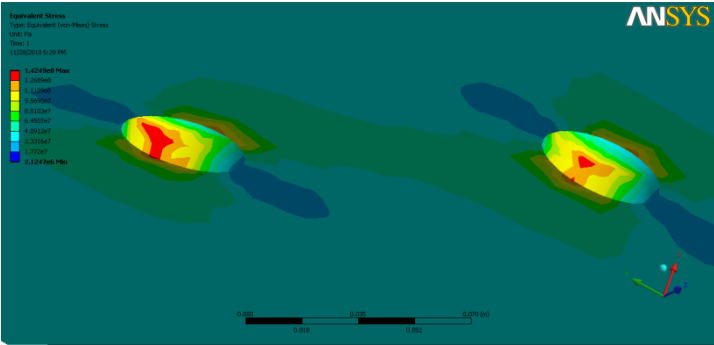
$L/d_n = 3.0$



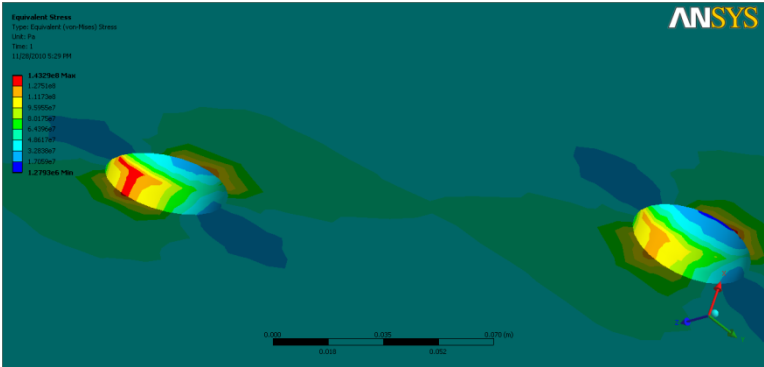
$L/d_n = 3.5$



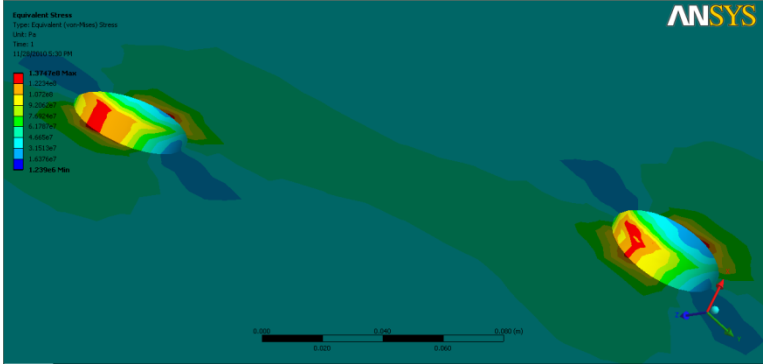
$$L/d_n = 4.0$$



$$L/d_n = 4.5$$



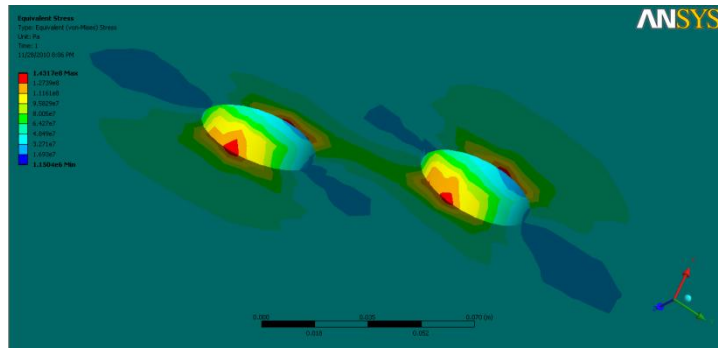
$$L/d_n = 5.0$$



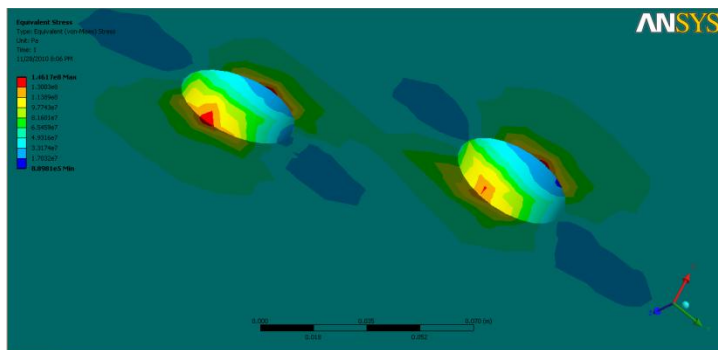
Example of simulation result for nozzles  $45^\circ$  from one another

**For  $r_n/t_n = 4$ ;**

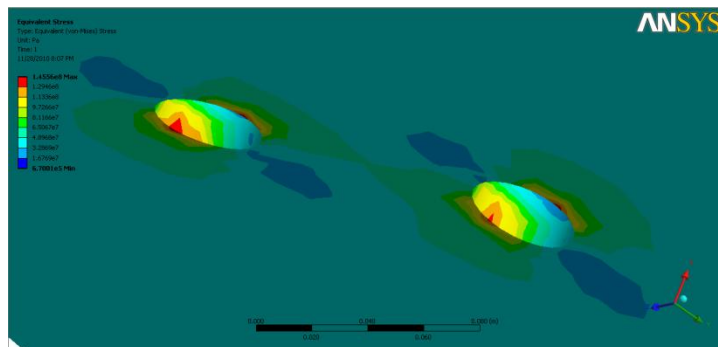
$L/d_n = 2.0$



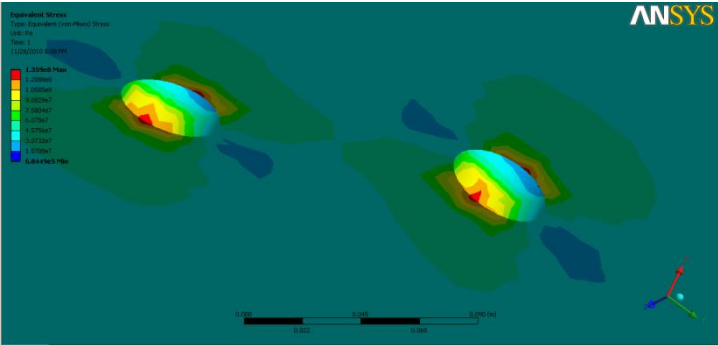
$L/d_n = 2.5$



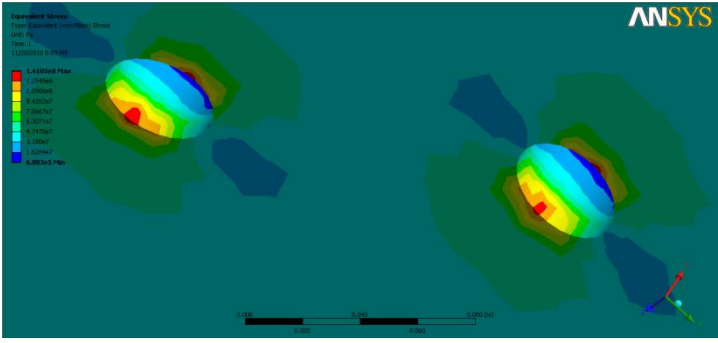
$L/d_n = 3.0$



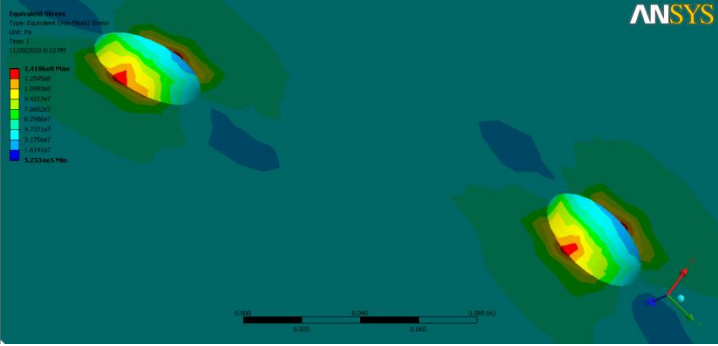
$$L/d_n = 3.5$$



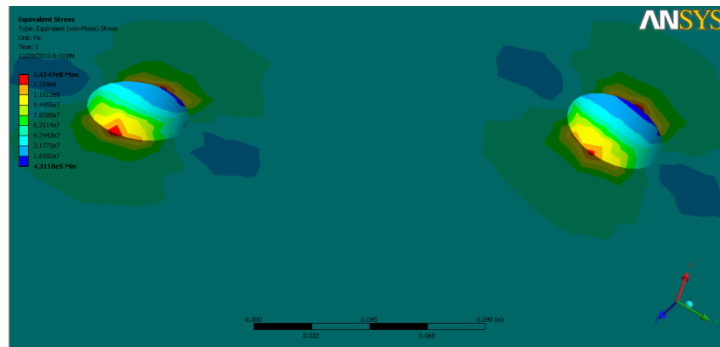
$$L/d_n = 4.0$$



$$L/d_n = 4.5$$

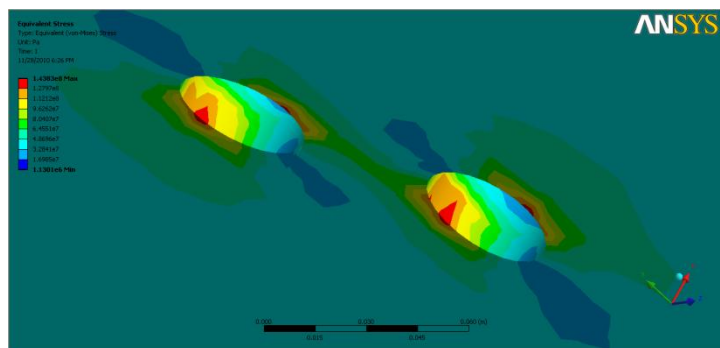


$$L/d_n = 5.0$$

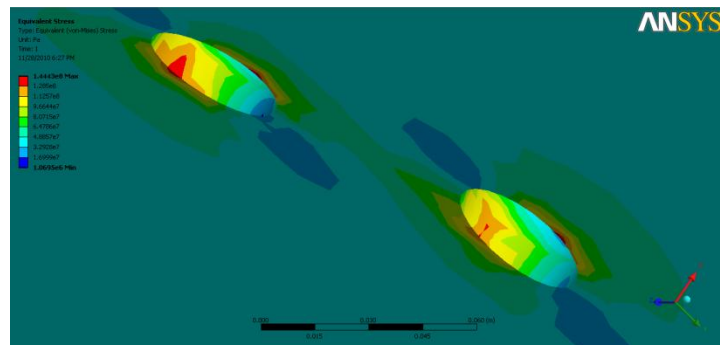


**For  $r_n/t_n = 5$ ;**

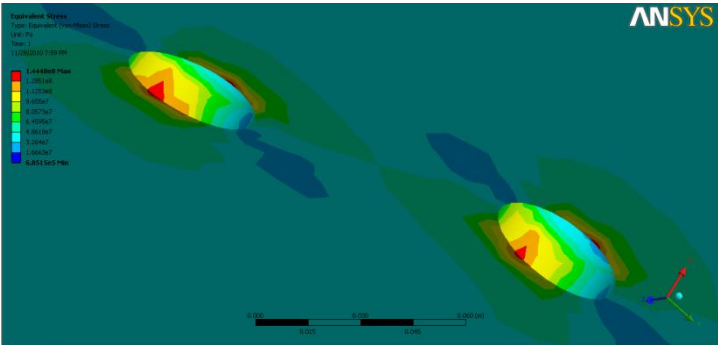
$$L/d_n = 2.0$$



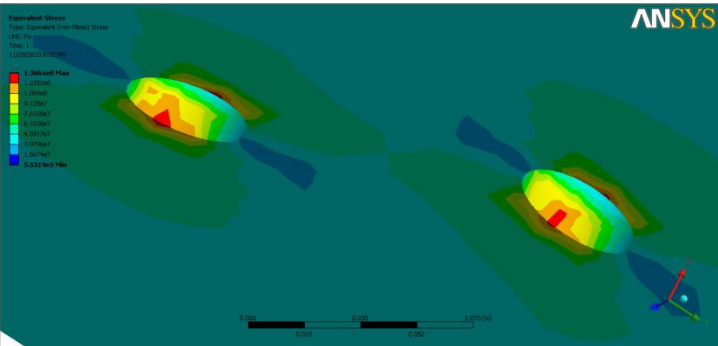
$$L/d_n = 2.5$$



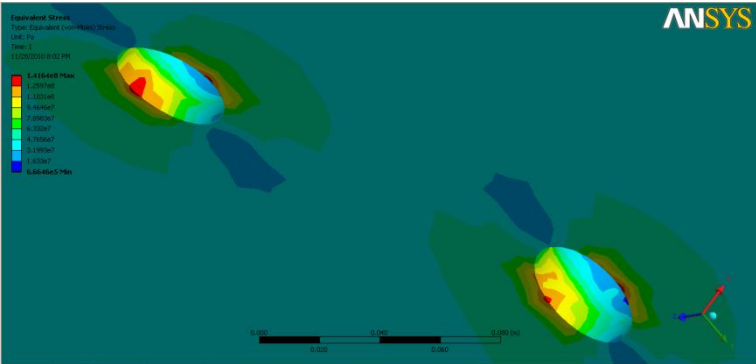
$$L/d_n = 3.0$$



$$L/d_n = 3.5$$

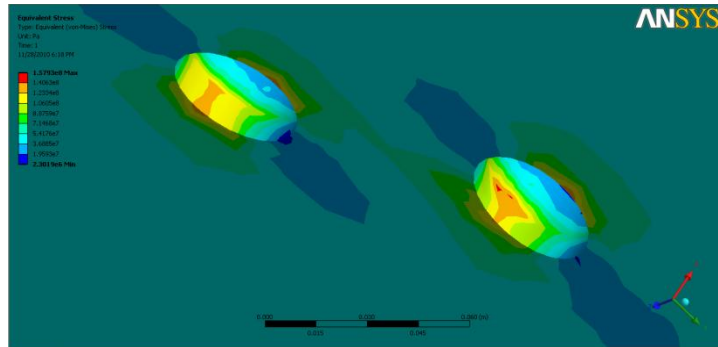


$$L/d_n = 4.0$$

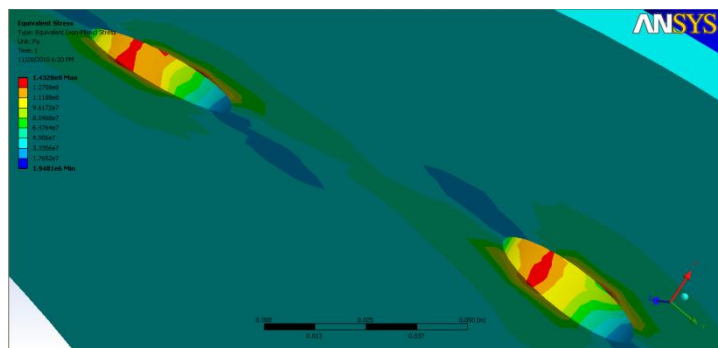




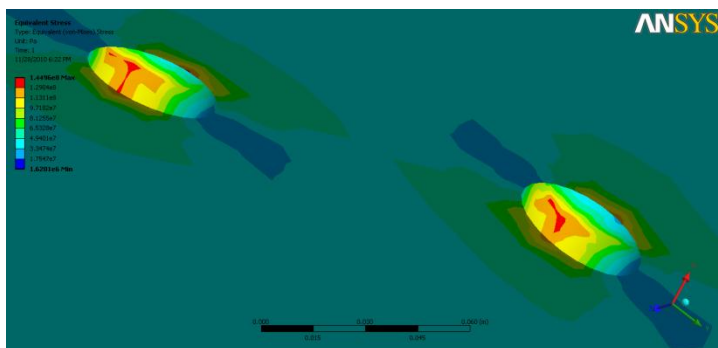
$$L/d_n = 2.5$$



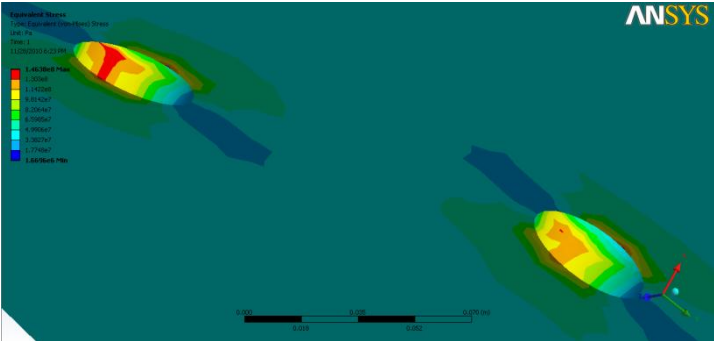
$$L/d_n = 3.0$$



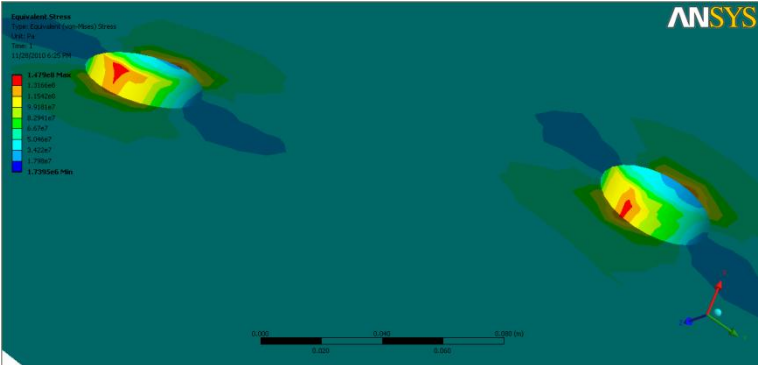
$$L/d_n = 3.5$$



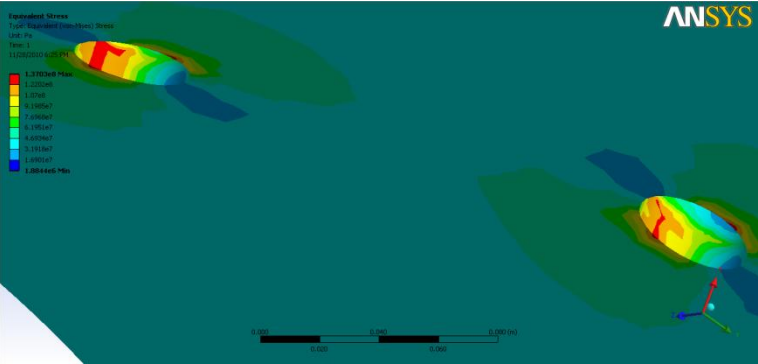
$L/d_n = 4.0$



$L/d_n = 4.5$



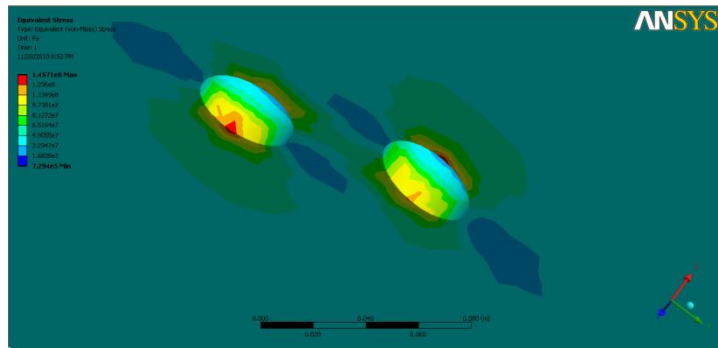
$L/d_n = 5.0$



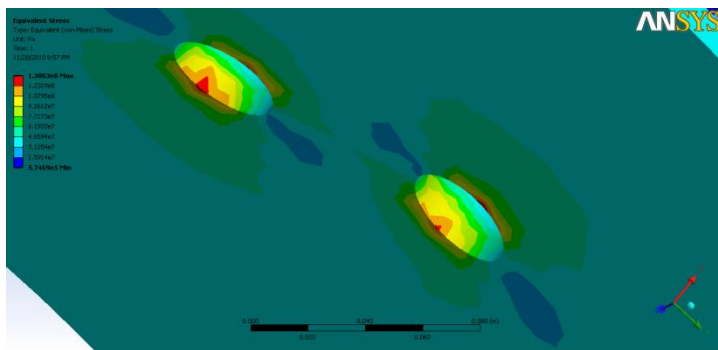
Example of simulation result for nozzles  $60^\circ$  from one another

**For  $r_n/t_n = 4$ ;**

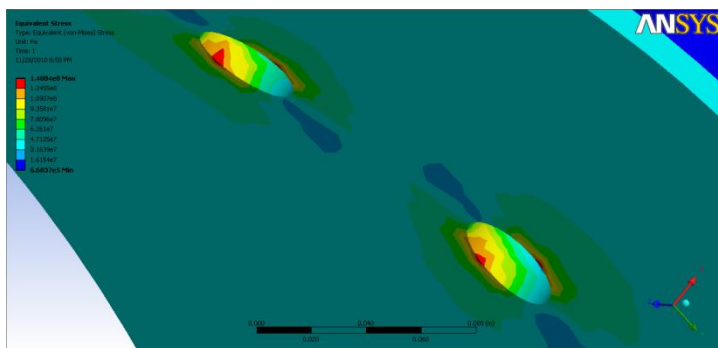
$L/d_n = 2.0$



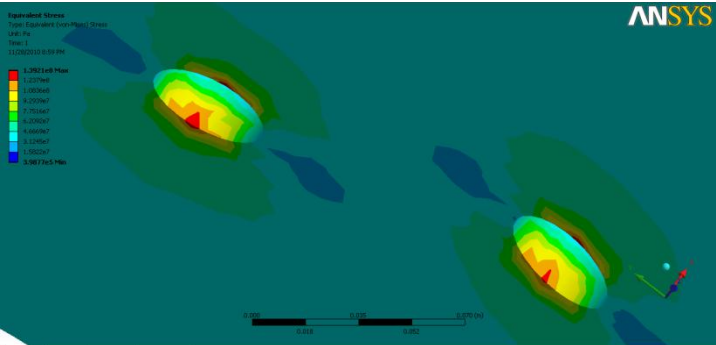
$L/d_n = 2.5$



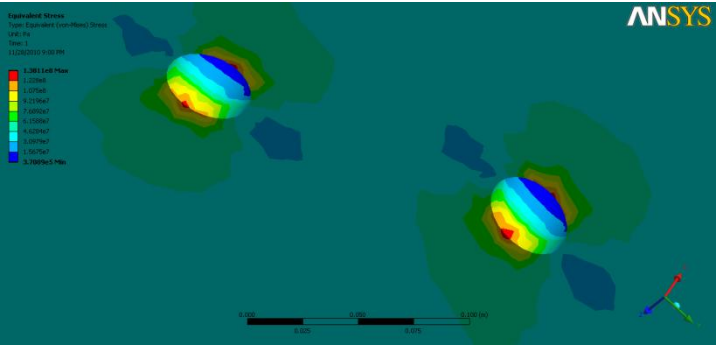
$L/d_n = 3.0$



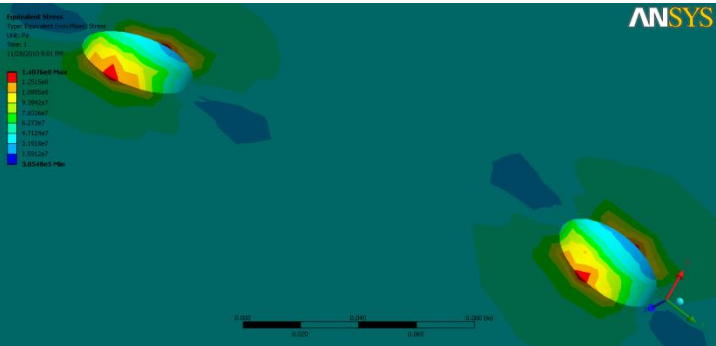
$$L/d_n = 3.5$$



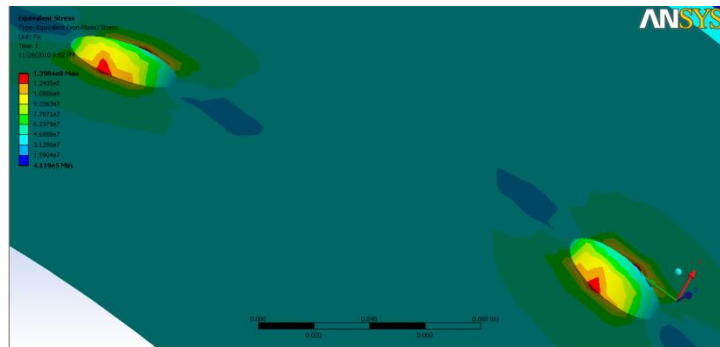
$$L/d_n = 4.0$$



$$L/d_n = 4.5$$

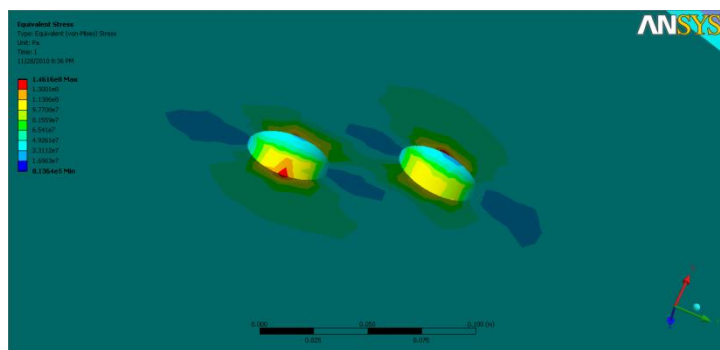


$$L/d_n = 5.0$$

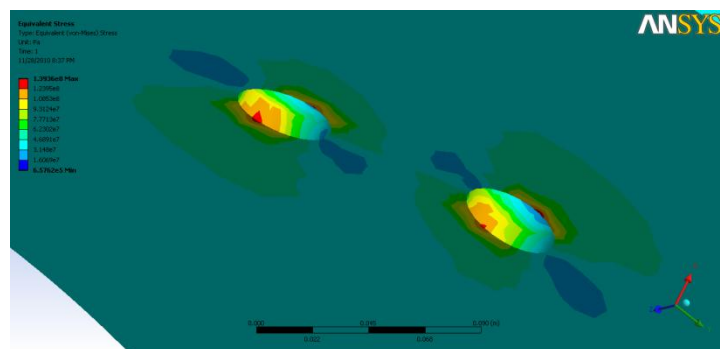


**For  $r_n/t_n = 5$ ;**

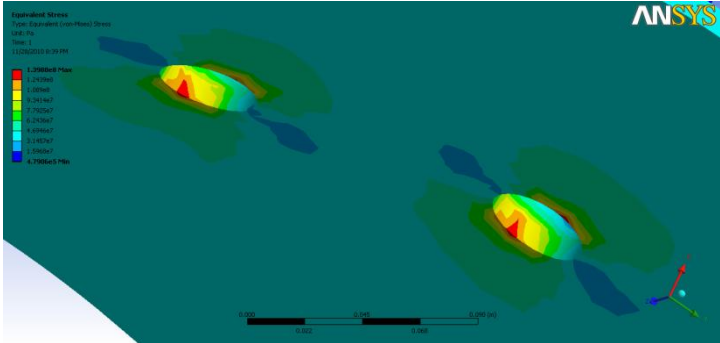
$$L/d_n = 2.0$$



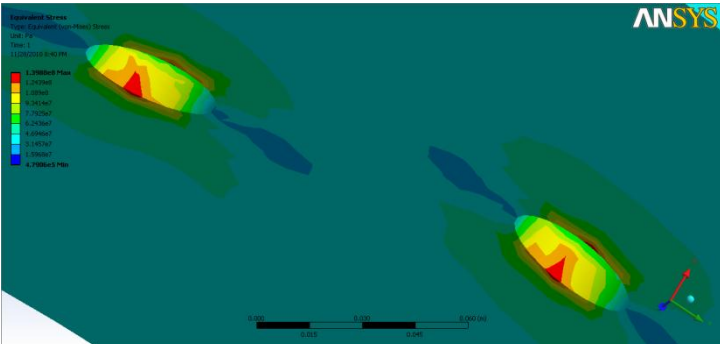
$$L/d_n = 2.5$$



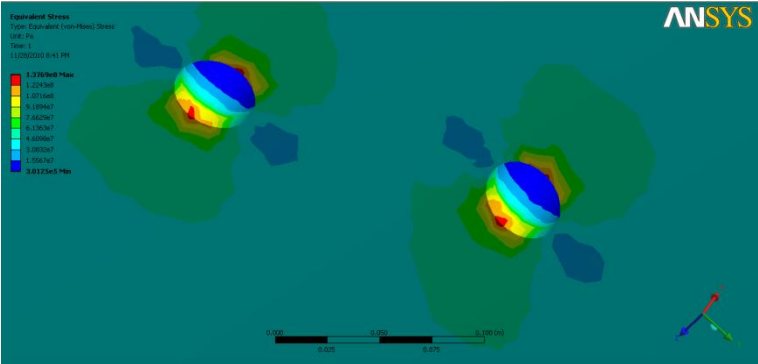
$$L/d_n = 3.0$$



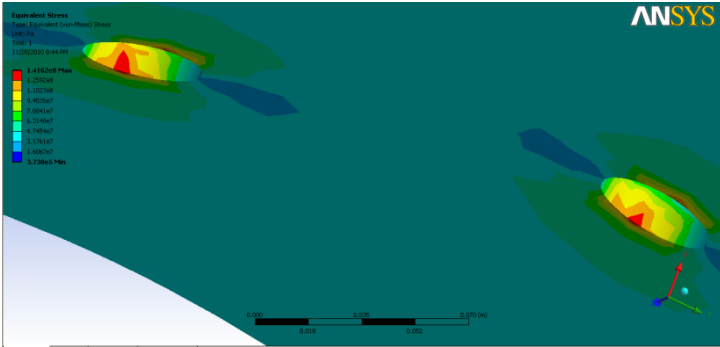
$$L/d_n = 3.5$$



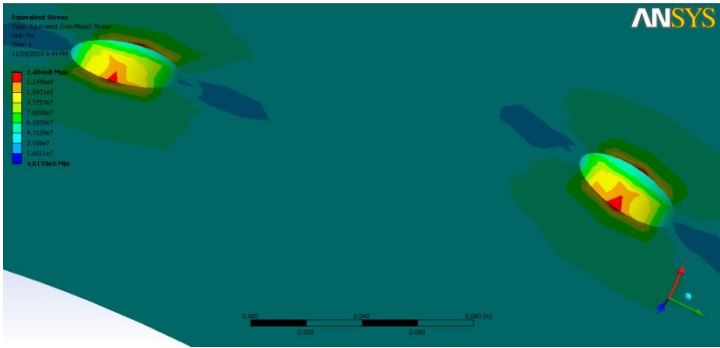
$$L/d_n = 4.0$$



$$L/d_n = 4.5$$

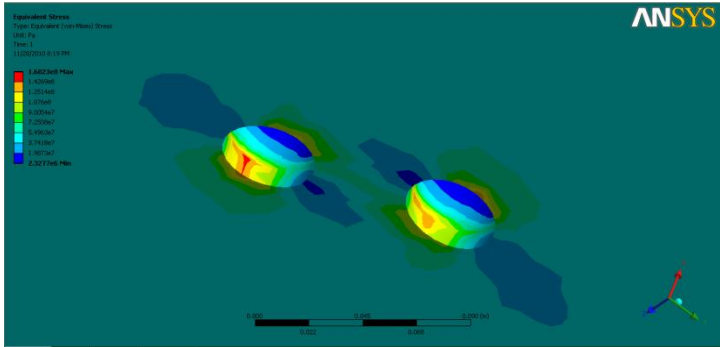


$$L/d_n = 5.0$$

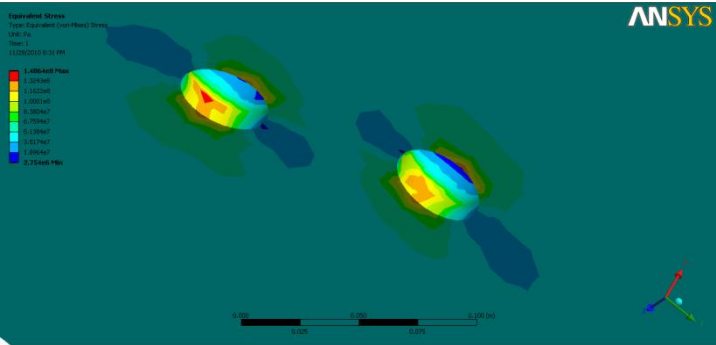


**For  $r_n/t_n = 10$**

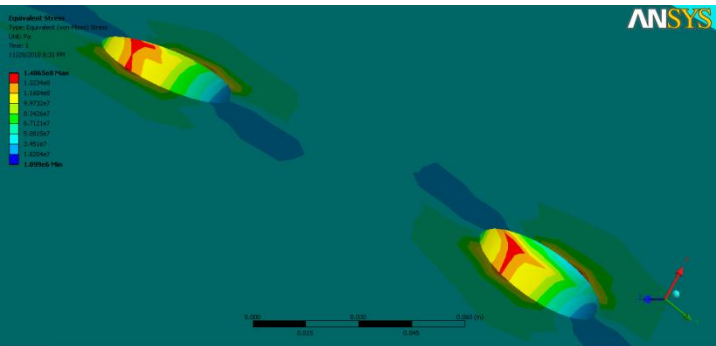
$$L/d_n = 2.0$$



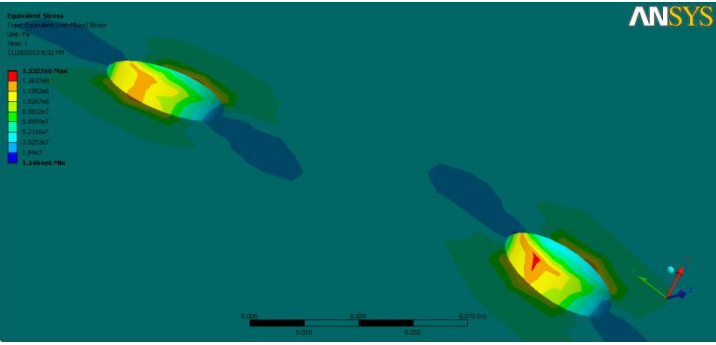
$$L/d_n = 2.5$$



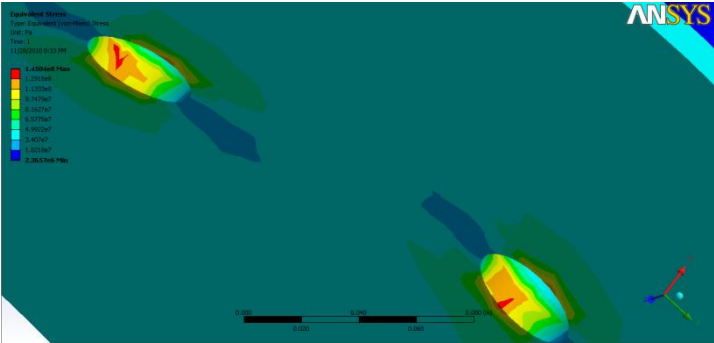
$$L/d_n = 3.0$$



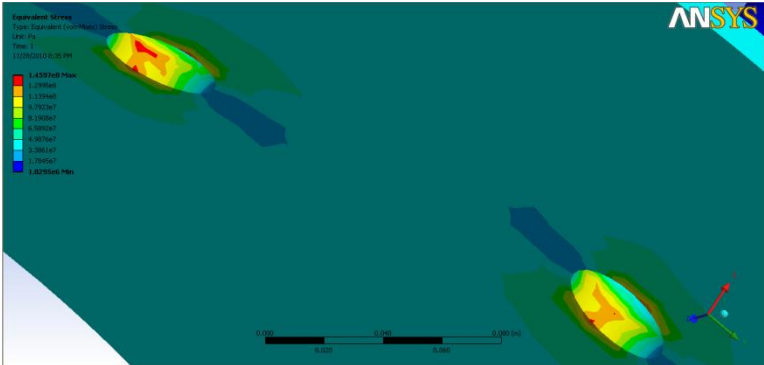
$$L/d_n = 3.5$$



$L/d_n = 4.0$



$L/d_n = 4.5$



$L/d_n = 5.0$

